Hierarchical Control of Internal Superstructure, Diameter, and Stability of Supramolecular and Macromolecular Columns Generated from Tapered Monodendritic Building Blocks

V. Percec,*,† D. Schlueter,† G. Ungar,‡ S. Z. D. Cheng,§ and A. Zhang§

The W.M. Keck Laboratories for Organic Synthesis, Department of Macromolecular Science, Case Western Reserve University, Cleveland, Ohio 44106-7202, Department of Engineering Materials and Center for Molecular Materials, University of Sheffield, Sheffield S1 3JD, U.K., and Maurice Morton Institute of Polymer Science, Department of Polymer Science, The University of Akron, Akron, Ohio 44325-3909

Received October 6, 1997; Revised Manuscript Received January 13, 1998

ABSTRACT: The synthesis of the first generation **AB_3** monodendrons 3,4,5-tris[6-alkyloxy-2-methylnaphthyloxy]benzoic acid (with decyl, dodecyl, tetradecyl, and hexadecyl alkyl groups), 3,4,5-tris[4-(4′-dodecyloxyphenyl)benzyloxy]benzoic acid, their ω-hydroxy(tetraethylene glycol) esters, and the corresponding methacrylates and poly(methacrylate)s is described. All monodendrons and the corresponding polymers self-assemble into supramolecular columns that self-organize in a columnar hexagonal (Φ_h) thermotropic liquid crystalline (LC) phase. The characterization of their Φ_h phase by a combination of differential scanning calorimetry (DSC), thermal optical polarized microscopy, and X-ray diffraction experiments demonstrated an intracolumnar microsegregated model for these supramolecular structures. The role and the contribution of the aliphatic, aromatic, oligooxyethylenic, and polymethacrylate fragments to the formation and the control of the external diameter, the internal structure, and the stability of these supramolecular columns and of the Φ_h phase were quantitatively evaluated and demonstrated that the contribution of the aromatic component dominates over that of the other structural components both in the control of column diameter and in thermodynamic stability of the resulted Φ_h phase.

Introduction

We are designing libraries of monodendrons which are employed as *exo*-receptors in the construction of flat tapered building blocks.[1−3] The structure of these monodendrons evolved from phasmidic and hemiphasmidic architectures.[1] These monodendrons are subsequently functionalized with *endo*-receptors, and the resulting building blocks self-assemble via a combination of various molecular recognition processes into supramolecular columns (Scheme 1), which self-organize in a two-dimensional hexagonal lattice.[1−3] Of particular interest are building blocks which generate supramolecular columns containing a channel formed from their *endo*-receptor(s) penetrating through the center of the column. Alternatively, when the *endo*-receptor of the same building block is replaced with a polymer backbone, the self-assembly of its own tapered side groups into a cylindrical shape induces a helical chain conformation of the polymer which penetrates the center of the column.[1b,c,f,g,h,3] This new approach to helical chain conformation is not dependent on backbone tacticity. These supramolecular columns are of interest for various potential applications such as unidirectional membranes, ionic, electronic, and photonic conductors, high modulus lightweight fibers, controlled release, gene transfer devices, etc. The design of cylindrical macromolecules via related principles has been and is being investigated in other laboratories.[4,5] However with the exception of the experiments reported from our laboratory,[1−3] no sufficient degree of perfection for the resulted cylindrical macromolecules to pack in a hexagonal lattice was accomplished.[4,5]

Scheme 1. Schematic Representation of the Self-Assembly of Flat-Tapered Monodendrons into Supramolecular Cylindrical Dendrimers and Subsequent Self-Organization of the Columnar Hexagonal (Φ_h) LC Assembly. The Structure for the Naphthalene-Substituted Monodendron Is Shown

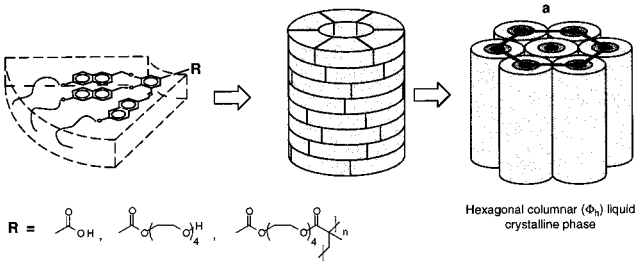

We are investigating strategies to control the diameter, internal superstructure, rigidity, and thermal stability of these nanocolumnar systems. Toward this goal, five synthetic variables are studied in our laboratory: (a) the structure of the repeat unit of a certain monodendron architecture; (b) the monodendron architecture based on a specific repeat unit; (c) the generation number of a homologous series of monodendrons obtained from identical repeat units and monodendron architecture; (d) the generation number of monodendrons obtained from a combination of different monodendron architectures based on identical repeat units; (e) the generation number of monodendrons obtained from a combination of different monodendron architectures and monodendron structural repeat units. Research in progress on all these strategies has shown that at least three additional structural options are available to the resulting monodendrons: (i) the flat tapered shape changes into a conical shape which produces a spherical supramolecule rather than a cylindrical one;

† Case Western Reserve University.
‡ University of Sheffield.
§ The University of Akron.

S0024-9297(97)01459-9 CCC: $15.00
Published on Web 03/04/1998

(ii) they exhibit a shape between flat tapered and flat disk-like which self-assembles into supramolecular cylinders, without forming a channel generated from their *endo*-receptors; (iii) they exhibit an undefined shape which produces an amorphous supramolecular material. The identification and characterization of the cylindrical and spherical supramolecular shapes generated by these building blocks is provided by the analysis of the thermotropic hexagonal columnar (Φ_h) (two-dimensional lattice) and cubic (Cu) (three-dimensional lattice) liquid crystalline (LC) phases in which they are self-organized. These experiments provide information on the mechanism of self-assembly in both solid and melt states.

The series of flat tapered monodendrons most investigated in our laboratory is based on 3,4,5-tris[alkyloxybenzyloxy]benzoate first generation monodendron (***n*ABG**),[1-3] where ***n*** stands for the number of carbon atoms in the aliphatic tail, **B** for benzyloxy and **G** for gallic acid. The goal of this publication is to report the synthesis and characterization of a new series of monodendrons based on the repeat unit in which the 1,4-phenylene group of the benzyl ether of ***n*ABG** was replaced with 1,4-biphenylene and 2,6-naphthylene. The alkyl tail length of the 2,6-naphthylene-functionalized monodendron was systematically varied from 10 to 16 methylene units. The resulting monodendrons were functionalized with a tetraethylene glycol *endo*-receptor which was subsequently attached to a polymethacrylate backbone. All resulting building blocks self-assemble into cylindrical shapes with channels containing a polymer backbone or an aggregate of *endo*-receptors. The analysis of the thermotropic Φ_h LC phase self-organized from these columns produced the first quantitative correlation between the stability of the supramolecular and macromolecular architecture and the structure of the monodendron manipulated via the variation of the aromatic part of the repeat unit while maintaining an identical monodendron architecture. Furthermore, the variation of alkyl tail length provided a method to demonstrate an intracolumnar microphase segregated structure containing an inner cylinder based on the *endo*-receptor(s) or the polymer backbone, surrounded by a rigid aromatic component, and an aliphatic outer sheath. The elucidation of the individual contributions of each of these segments will allow us to tailor the diameter, the internal superstructure, and the stability of the nanocolumn.

Results and Discussion

Synthesis of Monomers and Polymers. Scheme 2 outlines the synthesis of the five new first generation monodendrons **8-*n*-Nf**, where ***n*** represents the number of methylenic units in the alkyl tail, which is systematically varied from ***n*** = 10, 12, 14, 16, and of **8-12-Bp**. Scheme 3 describes the functionalization of these monodendrons with ω-hydroxy (tetraethylene glycol) to produce the building blocks **13-*n*-Nf** (***n*** = 10, 12, 14, 16), and **13-12-Bp** and their subsequent esterification with methacryloyl chloride to generate the methacrylate monomers **15-*n*-Nf** (***n*** = 10, 12, 14, 16), and **15-12-Bp**. The structure and purity of all compounds was determined by a combination of techniques including ^{1}H and ^{13}C NMR, IR, TLC, GC, HPLC, DSC, and thermal optical polarized microscopy. The first step from this sequence of reactions involved the acid-catalyzed esterification of the commercially available 2-hydroxy-6-naphthoic acid with EtOH to give ethyl 6-hydroxy-2-naphthoate (**2-Nf**) in 94% yield. Methyl 4-(4′-Hydroxyphenyl) benzoate (**2-Bp**) was synthesized as described previously.[6] Etherification of **2-Nf** with bromododecane was accomplished using anhydrous K_2CO_3 in DMF at 70 °C to yield ethyl 6-(dodecyloxy)-2-naphthoate (**3-12-Nf**) in 62% yield following recrystallization from EtOH. Identical reaction conditions were used for the synthesis of the 10, 14, and 16 carbon alkyl chain analogues, **3-10-Nf** (76%), **3-14-Nf** (88%), and **3-16-Nf** (84%). Methyl 4-[4′-(dodecyloxy)phenylbenzoate (**3-12-Bp**) was synthesized in 79% yield under the same conditions with **3-*n*-Nf**, starting from methyl 4-(4′-hydroxyphenyl)benzoate (**2-Bp**) and bromododecane. Unlike the naphthoate esters **3-*n*-Nf** (***n*** = 10, 12, 14, 16), **3-12-Bp** exhibits a monotropic LC phase. Quantitative ester reduction was accomplished for all **3-*n*-Ar** compounds using identical reaction conditions, i.e., $LiAlH_4$ in Et_2O at 0−5 °C with acidic workup, to give the corresponding alcohols **4-*n*-Nf** (***n*** = 10, 12, 14, 16) and **4-12-Bp** in 78−94% isolated yield. $LiAlH_4$ provided a convenient and efficient method to reduce this series of esters. Chlorination of the resulting series of alcohols with $SOCl_2$ in CH_2Cl_2 containing a catalytic amount of DMF was quantitative (>99%) and the resulting chloromethylnaphthalenes **5-*n*-Nf** (***n*** = 10, 12, 14, 16) and benzyl chloride **5-12-Bp** were used without further purification. Alkylation of methyl 3,4,5-trihydroxybenzoate (**6**) with 6-(dodecyloxy)-2-(chloromethyl)naphthalene (**5-12-Nf**) was performed using anhydrous K_2CO_3 in DMF at 70 °C. Purification by a combination of column chromatography (Al_2O_3, CH_2Cl_2 eluent) and recrystallization from acetone afforded methyl 3,4,5-tris[(6-(dodecyloxy)-naphth-2-yl)methoxy]benzoate (**7-12-Nf**) in 69% yield. The other taper-shaped building blocks were synthesized under identical conditions to yield **7-10-Nf** (86%), **7-14-Nf** (87%), **7-16-Nf** (63%), and **7-12-Bp** in 50% yield. The low yield of **7-12-Bp** was presumably due to its poor solubility in DMF at 70 °C. Basic hydrolysis of the methyl ester group of **7-*n*-Nf** (***n*** = 10, 12, 14, 16) was accomplished using KOH in 4:1 EtOH/*i*-PrOH at 80 °C to produce the corresponding benzoic acids **8-10-Nf** (95%), **8-12-Nf** (94%), **8-14-Nf** (89%), and **8-16-Nf** (81%). The monodendron **7-12-Bp** was hydrolyzed with KOH in refluxing *i*-PrOH using a catalytic amount of tetrabutylammonium hydrogen sulfate (TBAH) as phase transfer catalyst to yield **8-12-Bp** (96%) following recrystallization from methyl ethyl ketone.

tert-Butyldimethylsilyl (TBDMS) monoprotected tetraethylene glycol was used in the esterification of the benzoic acid monodendrons **8-*n*-Nf** (***n*** = 10, 12, 14, 16) and **8-12-Bp**. This strategy is similar to the previously published procedure used for the allyl ether monoprotected tetraethylene glycols.[1b,c] 2-{2-[2-(2-(*tert*-Butyldimethylsiloxy)ethoxy)ethoxy]ethoxy}ethanol (**11**) was synthesized from *tert*-butyldimethylsilyl chloride (**10**) using an excess of tetraethylene glycol (**9**) in dry DMF and resulted in a 92% yield of a mixture of 92.2% monoprotected tetraethylene glycol and 7.8% of diprotected tetraethylene glycol. A literature procedure was adapted for this reaction.[7] The unreacted tetraethylene glycol was removed by repeated extraction of the $CHCl_3$ solution of the crude product with H_2O. The TBDMS protective group was chosen for both its ease of introduction[7] and its ability to be selectively cleaved under mild conditions in the presence of benzyl ethers using a fluoride ion source (HF/Py).[8] In contrast, the conditions necessary to cleave an allyl ether protective group

Scheme 2. Synthesis of 3,4,5-tris-[*n*-alkyloxy]benzoic Acid Derivatives, 8-*n*-Nf (*n* = 10, 12, 14, 16) and 8-12-Bp

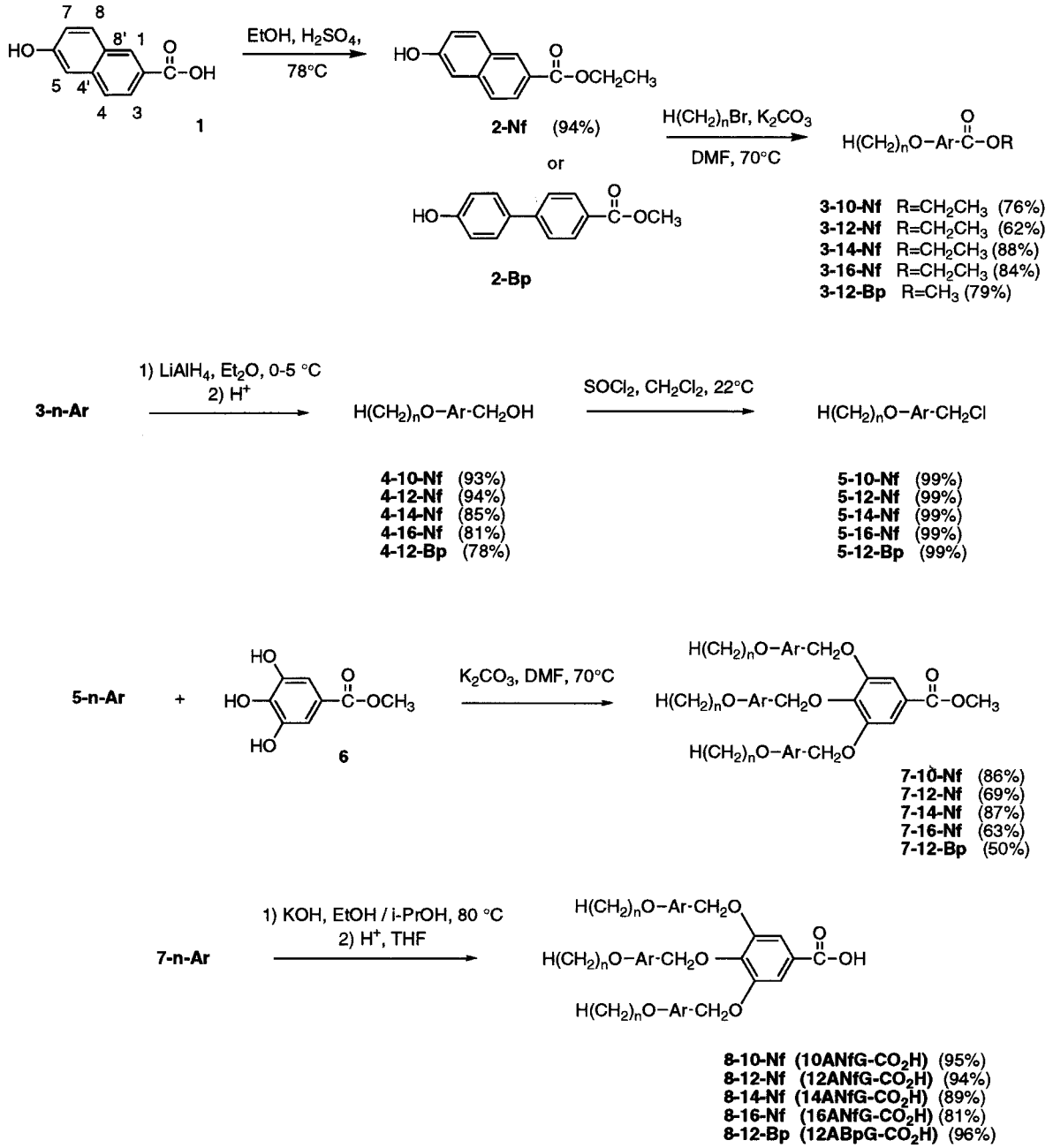

were not compatible with the benzyl ether based repeat units. These modified conditions allow for convenient purification of the crude esterification product by column chromatography. Neutral conditions were chosen for the esterification (DCC, DPTS) of the benzoic acid monodendrons **8-*n*-Nf** (***n*** = 10, 12, 14, 16) and **8-12-Bp** with TBDMS monoprotected tetraethylene glycol (**11**). The esterification of **8-*n*-Nf** (***n*** = 10, 12, 14, 16) was accomplished in refluxing CH_2Cl_2 followed by purification by column chromatography (Al_2O_3, 3:1 hexanes/ethyl acetate) to afford **12-10-Nf** (60% yield), **12-12-Nf** (64% yield), **12-14-Nf** (66% yield), and **12-16-Nf** (78% yield). The less soluble **8-12-Bp** was esterified in refluxing 1,2-dichloroethane and purified by column chromatography (Al_2O_3, CH_2Cl_2 eluent) to give **12-12-Bp** in 52% yield after recrystallization from acetone. Quantitative deprotection of the TBDMS group was conveniently performed using HF/Py in THF at 0−5 °C with no evidence of benzyl ether cleavage and resulted in yields ranging from 71 to 99% after recrystallization. The alcohols **13-*n*-Nf** (***n*ANfG-4EO-OH**, ***n*** = 10, 12, 14, 16) and **13-12-Bp** (***n*ABpG-4EO-OH**) were then esterified with methacryloyl chloride using Et_3N in CH_2Cl_2 at 0−5 °C to produce the methacrylate monomers **15-*n*-Nf** (***n*** = 10, 12, 14, 16) and **15-12-Bp** in 45 to 52% yield after purification by column chromatography (Al_2O_3, 2:1 hexanes/ethyl acetate).

Polymerization of the resulting methacrylates was performed at 60 °C in benzene (33 wt %) using 1.0 wt % of AIBN as radical initiator. The resulting polymethacrylates **16-*n*-Nf** (***n*** = 10, 12, 14, 16) (***n*ANfG-4EO-PMA**) and **16-12-Bp** (**12ABpG-4EO-PMA**), were obtained in 44 to 80% yield after purification by column chromatography (Al_2O_3, hexanes eluent to remove the residual monomer), and precipitation into methanol. Their molecular weights ($\bar{M}_n$) and polydispersities ($\bar{M}_w/\bar{M}_n$) are listed in Table 1.

Scheme 3. Synthesis of Methacrylate Derivatives 15-*n*-Nf (*n* = 10, 12, 14, 16) and 15-12-Bp and Their Polymerization to 16-*n*-Nf (*n*ANfG-4EO-PMA) (*n* = 10, 12, 14, 16) and 16-12-Bp (12ABpG-4EO-PMA)

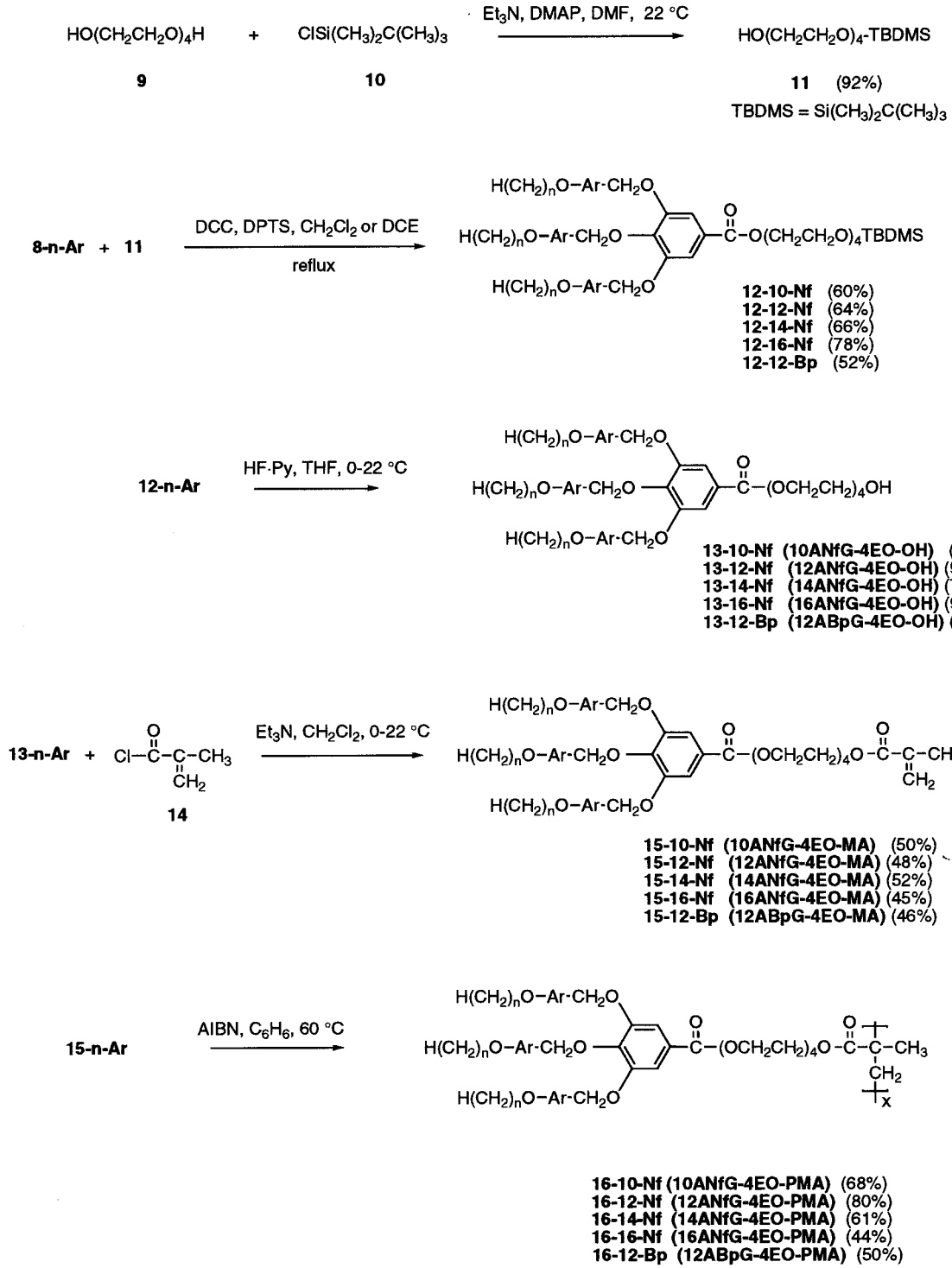

Thermal and Structural Analysis. The thermal behavior and structural characterization of monodendrons **8-*n*-Nf** (***n*** = 10, 12, 14, 16), **8-12-Bp**, ***n*ANfG-4EO-OH** (**13-*n*-Nf**, ***n*** = 10, 12, 14, 16), **12ABpG-4EO-OH** (**13-12-Bp**) and polymethacrylates ***n*ANfG-4EO-PMA** (**16-*n*-Nf**, ***n*** = 10, 12, 14, 16) and **12ABPG-4EO-PMA** (**16-12-Bp**) were performed by a combination of differential scanning calorimetry (DSC), X-ray diffraction, and thermal optical polarized microscopy. The results are summarized in Tables 1 and 2. All benzoic acids **8-*n*-Nf** (***n*** = 10, 12, 14, 16) (***n*ANfG-CO$_2$H**) and **8-12-Bp** (**12ABpG-CO$_2$H**) display a Φ_h LC phase. By comparison with the parent tribenzyloxybenzoic acid (**12ABG**),[1f] the larger phenyl ether substituents significantly stabilize both the crystalline and Φ_h LC phases exhibited by **8-*n*-Nf**. For **10ANfG-CO$_2$H** (**8-10-Nf**) the crystalline melting ($T_{k-\Phi h}$) increased by 41 °C and the isotropization ($T_{\Phi h-i}$) increased by 57 °C with respect to that of the tribenzyloxybenzoic acid **12ABG**.[1f] The longer alkyl tail naphthyloxy analogues ***n*ANfG-CO$_2$H** (**8-*n*-Nf**, ***n*** = 12, 14, 16) display a similar behavior. The stabilization of the Φ_h phase was more pronounced for the biphenyl-substituted monodendron **12ABpG-CO$_2$H** (**8-12-Bp**), where the $T_{k-\Phi h}$ increased by 71 °C and the

Table 1. Characterization of *n*ANfG-CO_2H (8-*n*-Nf, *n* = 10, 12, 14, 16), 12ABpG-CO_2H (8-12-Bp), *n*ANfG-4EO-OH (13-*n*-Nf, *n* = 10, 12, 14, 16), 12ABpG-4EO-OH (13-12-Bp), *n*ANfG-4EO-PMA (16-*n*-Nf, *n* = 10, 12, 14, 16), and 12ABpG-4EO-PMA (16-12-Bp) with Data Collected from the First Heating and Cooling DSC Scans on the First Line and Data from the Second Heating Scan on the Second Line (k = Crystalline Phase, Φ_h = Hexagonal Columnar LC Phase, I = Isotropic Phase)

compound	yield[a] (%)	M_n (GPC)	M_w/M_n (GPC)	thermal transitions (°C) and corresponding enthalpy changes (kcal/mol or kcal/mru) heating	cooling
10ANfG-CO_2H	95			k 112 (3.22), Φ_h 200 (3.45), i[b]	
12ANfG-CO_2H	94			k 106 (3.07), Φ_h 200 (3.52), i[b]	
14ANfG-CO_2H	89			k 69 (6.91), k 106 (3.64), Φ_h 201 (4.50), i[b]	
16ANfG-CO_2H	81			k 69 (12.24), k 102 (3.10), Φ_h 198 (3.89), i[b]	
12ABpG-CO_2H	76			k 142 (8.26), Φ_h 219 (0.96), i[b]	
10ANfG-4EO-OH	72			k 65 (10.1), Φ_h 82 (1.37), i k_1 36 (3.87), k_2 52 (−5.36), k_3 67 (10.25), Φ_h 82 (1.19), i	i 78 (1.18), Φ_h 40 (4.26), k_1 21 (3.24), k_2
12ANfG-4EO-OH	95			k 65 (15.8), Φ_h 88 (1.28), i k_1 46 (−1.23), k_2 66 (13.4), Φ_h 87 (1.21), i	i 83 (1.34), Φ_h 38, 29 (13.0),[c] k
14ANfG-4EO-OH	71			k 68 (10.8), Φ_h 93 (1.48), i k 69 (13.8), Φ_h 94 (1.22), i	i 90 (1.20), Φ_h 39 (14.6), k
16ANfG-4EO-OH	99			k_1 37 (5.05), k_2 69 (15.6), Φ_h 104 (0.64), i k 47, 71 (16.0), Φ_h 104 (0.68), i[d]	i 99 (0.63), Φ_h 41 (12.7), k
12ABpG-4EO-OH	94			k_1 101 (2.9), k_2 104 (−3.64), k_3 113 (14.3), i k 101, 112 (18.7), i[d]	i 94 (16.8), k
10ANfG-4EO-PMA	68	78 300	1.5	g 28, Φ_h 139 (0.45), i g 23, Φ_h 139 (0.47), i	i 129 (0.44), Φ_h 19, g
12ANfG-4EO-PMA	80	32 500	2.0	g 32, Φ_h 149 (0.45), i g 23, Φ_h 148 (0.44), i	i 142 (0.48), Φ_h 20, g
14ANfG-4EO-PMA	61	22 600	1.4	k 41 (6.63), Φ_h 153 (0.37), i Φ_h 152 (0.46), i	i 147 (0.39), Φ_h
16ANfG-4EO-PMA	44	20 200	1.3	k 35 (10.7), Φ_h 154 (0.45), i k 34 (8.03), Φ_h 152 (0.48), i	i 147 (0.39), Φ_h 25 (6.24), k
12ABpG-4EO-PMA	50	140 600	2.9	k 70 (3.89), Φ_h 176 (0.33), i k 71 (2.50), Φ_h 179 (0.14), i	i 169, Φ_h 57 (3.54), k

[a] Isolated. [b] Decomposition. [c] Heating to 120 °C. [d] Combined enthalpy.

Table 2. Characterization of *n*ANfG-CO_2H (8-*n*-Nf, *n* = 10, 12, 14, 16), 12ABpG-CO_2H (8-12-Bp), *n*ANfG-4EO-OH (13-*n*-Nf, *n* = 10, 12, 14, 16), 12ABpG-4EO-OH (13-12-Bp), *n*ANfG-4EO-PMA (16-*n*-Nf, *n* = 10, 12, 14, 16), and 12ABpG-4EO-PMA (16-12-Bp) by X-ray Diffraction Experiments

compound	temp (°C)	d_{100} (Å)	$\langle d_{100}\rangle$[a] (Å)	d_{110} (Å)	d_{200} (Å)	a[b] (Å)	R[b] (Å)	S[b] (Å)	ρ[c](g/mL)	μ[d]
10ANfG-CO_2H	130	36.9	36.9	21.2	18.5	42.6	21.3	24.6		
12ANfG-CO_2H	130	38.5	38.6	22.4	19.3	44.6	22.3	25.7		
14ANfG-CO_2H	130	41.3	41.0[f]		20.3	47.3	23.7	27.3		
16ANfG-CO_2H	130	42.5	42.3[f]		21.0	48.8	24.4	28.2		
12ABpG-CO_2H		42.7				49.3[g]				
10ANfG-4EO-OH	72	49.6	49.6	28.7	24.7	57.3	28.7	33.1		
12ANfG-4EO-OH	72	52.3	52.3	30.2	26.1	60.4	30.2	34.8		
14ANfG-4EO-OH	72	51.4	52.4	30.7	26.3	60.5	30.3	34.9		
16ANfG-4EO-OH	72	53.2	54.1	32.1	26.8	62.5	31.3	36.1		
10ANfG-4EO-PMA	72	53.4	53.6	31.0	26.8	61.9	31.0	35.7	1.09	6.2
12ANfG-4EO-PMA	72	56.5	56.4	32.5	28.2	65.1	32.6	37.6	1.05	6.3
14ANfG-4EO-PMA	72	57.8	57.8	33.2	29.1	66.7	33.4	38.5	1.03	6.1
16ANfG-4EO-PMA	72	58.9	60.6	35.9	30.3	70.0	35.0	40.4	1.01	6.2
12ABpG-4EO-PMA	55	61.0	60.0[e]	34.1		69.3	34.7	40.0	1.09	7.0

[a] $\langle d_{100}\rangle = [d_{100} + d_{110}\sqrt{3} + 2d_{200}]/3$. [b] $a = 2\langle d_{100}\rangle/\sqrt{3}$; $R = \langle d_{100}\rangle/\sqrt{3}$; $S = 2R/\sqrt{3}$. [c] ρ = density at 20 °C. [d] Number of taper-shaped units per column layer, $\mu = 3\sqrt{3}N_AS^2d\rho/2M$. [e] $\langle d_{100}\rangle = [d_{100} + d_{110}\sqrt{3}]/2$. [f] $\langle d_{100}\rangle = [d_{100} + 2d_{200}]/2$. [g] $a = 2d_{100}/\sqrt{3}$.

$T_{\Phi h-i}$ increased by 76 °C. Undoubtedly, the stability of the crystalline phase is enhanced by the increased rigidity and decreased conformational freedom imparted by the arenealkyloxy groups. The column diameter (a, Å) determined by X-ray diffraction experiments increases with the length of the alkyloxy tail. The monodendron **10ANfG-CO_2H** (**8-10-Nf**) (a = 42.6 Å) shows roughly the same column diameter as the parent **12ABG** (a = 42.9 Å).[9] This result is not unexpected, provided the number of monodendrons per column cross section (μ) is the same, since the length of the extended chain conformation of the (*p*-(dodecyloxy)benzyl)oxy and (6-(decyloxy)-2-methylenenaphthyl)oxy tails are identical, i.e., 20.3 Å. However, the thermal stabilities of their Φ_h LC phase are remarkably different, indicating the significant contribution of the aromatic component to the stabilization of the resulted supramolecular architecture. The longer alkyl chain analogues show an increase in the column diameter with increasing chain lengths from 44.6 Å for **12ANfG-CO_2H** (**8-12-Nf**) to 47.3 Å for **14ANfG-CO_2H** (**8-14-Nf**) and to 48.8 Å for **16ANfG-CO_2H** (**8-16-Nf**) (Table 2).

The tetraethylene glycol derivatives, **10ANfG-4EO-OH** (**13-10-Nf**) and **12ANfG-4EO-OH** (**13-12-Nf**), show a crystalline and an enantiotropic Φ_h LC phase. An increase in the stability of both phases is observed on comparing to the corresponding tribenzyloxy tetraethylene glycol (**12ABG-4EO-OH**).[1f] Inserting a naphthyloxy with a decyloxy tail (**10ANfG-4EO-OH**) increases the $T_{k-\Phi h}$ by 18 °C and the $T_{\Phi h-i}$ by 25 °C. For the

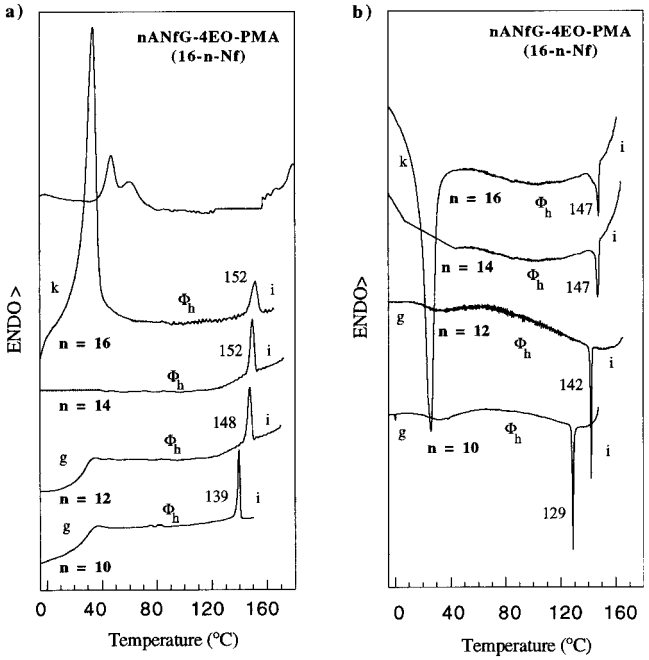

Figure 1. DSC traces of (a) second heating and (b) first cooling scans of the ***n*ANfG-4EO-PMA** polymethacrylate series (***n*** = 10, 12, 14, 16).

analogous dodecyloxy monodendron (**12ANfG-4EO-OH**) the $T_{k-\Phi h}$ increases by 17 °C and the $T_{\Phi h-i}$ increases by 30 °C. The longer alkyl chain analogues show a similar trend. The $T_{k-\Phi h}$ for **14ANfG-4EO-OH** (**13-14-Nf**) increases by 20 °C relative to **12ABG-4EO-OH**, and its $T_{\Phi h-i}$ increases by 37 °C. For **16ANfG-4EO-OH** (**13-16-Nf**), the $T_{k-\Phi h}$ increases by 22 °C and $T_{\Phi h-i}$ increases by 47 °C, relative to **12ABG-4EO-OH**. The continual increase in the thermal stability of the Φ_h phase in this series follows the increase in the ratio of the aliphatic to both aromatic and oligooxyethylene components. The bulky naphthyl group contributes to the suppression of the crystallization of the monodendron based on even the longest alkyl tail. X-ray diffraction experiments show a systematic increase in the column diameter from 53.2 Å for the parent **12ABG-4EOH**[1f] to 57.3 Å for **10ANfG-4EO-OH**, 60.3 Å for **12ANfG-4EO-OH**, 60.5 Å for **14ANfG-4EO-OH**, and 62.5 Å for **16ANfG-4EO-OH**. Inserting a biphenyl substituent (**12ABpG-4EO-OH**) increases the crystallizability sufficiently to override the Φ_h phase induced by such a weak *endo*-receptor, and the compound shows only crystalline melting endotherms at 101 and 112 °C (Table 1).

All polymethacrylates, ***n*ANfG-4EO-PMA** (**16-*n*-Nf**, ***n*** = 10, 12, 14, 16) and **12ABpG-4EO-PMA** (**16-12-Bp**), display an enantiotropic Φ_h LC phase with varying thermal stability. DSC traces for the ***n*ANfG-4EO-PMA** (***n*** = 10, 12, 14, 16) series are presented in Figure 1. In each case, the $T_{\Phi h-i}$ transition is sharp and the degree of supercooling of $T_{i-\Phi h}$ is low, which indicates thermodynamically controlled self-assembling and self-organization processes. Comparison to the corresponding tribenzyloxy polymethacrylate (**12ABG-4EO-PMA**) ($T_{\Phi h-i}$ = 99 °C)[1f] shows a dramatic increase in the stability of the supramolecular structure on changing the aromatic substituent. Inserting a naphthalene aromatic substituent into these polymethacrylates increases the thermal stability of the Φ_h mesophase by 40 and 49 °C for the **10ANfG-4EO-PMA** (**16-10-Nf**) and **12ANfG-4EO-PMA** (**16-12-Nf**) polymethacrylates, respectively. The longer alkyl chain compounds show an even larger increase in the stability of the Φ_h mesophase. The isotropization temperature increases by 53 °C for both **14ANfG-4EO-PMA** (**16-14-Nf**) and **16ANfG-4EO-PMA** (**16-16-Nf**). Additionally, a crystalline melting at 34 °C is observed for the **16ANfG-4EO-PMA** derivative. Inserting a biphenyl aromatic substituent **12ABpG-4EO-PMA** (**16-12-Bp**) induces a crystalline phase ($T_{k-\Phi h}$ = 71 °C) and increases the stability of the Φ_h LC phase of the polymethacrylate by 80 °C (Table 1).

The column diameter of polymethacrylates shows a systematic dependence on the nature of the monodendron aromatic component and on the length of their alkyloxy tail. The polymethacrylate **12ABG-4EO-PMA** has a column diameter (*a*) of 57.2 Å.[1f] Replacing its benzyl ethers with naphthyl methyl ether substituent increases the column diameter of the polymethacrylate to 65.2 Å for **12ANfG-4EO-PMA** (**16-12-Nf**). A biphenyl methyl ether (**12ABpG-4EO-PMA**, **16-12-Bp**) increases the column diameter still further to 69.3 Å (Table 2). Increasing the length of the alkyloxy tail also leads to an increase in the column breadth. For each class of naphthyloxy substituted compounds paired with different *endo*-receptors (**8-*n*-Nf**, **13-*n*-Nf**, and **16-*n*-Nf**), the column diameter increased on increasing the length of the aliphatic tail for each compound in the series. For example, in the polymethacrylate series, the naphthalene monodendron with a 10 carbon alkyl tail (**10ANfG-4EO-PMA**) displayed a column diameter (*a*) of 61.9 Å. The remainder of the series showed a regular increase in the column diameter as a function of alkyloxy tail length from 65.1 Å for **12ANfG-4EO-PMA** (**16-12-Nf**) to 66.7 Å for **14ANfG-4EO-PMA** (**16-14-Nf**) and to 70.0 Å for **16ANfG-4EO-PMA** (**16-16-Nf**) (Table 2).

Intracolumnar Model of the Supramolecular and Macromolecular Columns. The influence of the length of the aryl methyl ether (R_{calc}) on the stability of the Φ_h phase and the diameter of the columns for the **12ARG-4EO-PMA** (**16-12-Ar**) are plotted in Figure 2a. An increase in R_{calc} of the aryl methyl ether aromatic component (*R*) of the monodendron leads to a stabilization of the resulting supramolecular structure. This is indicated by the increase in isotropization temperature ($T_{\Phi h-i}$) when **R** changes from O, to B, to Nf and to Bp. This stability increase results from the increase in the diameter and the aromatic character of the column core. A linear increase in the diameter of the supramolecular column is observed with the increase of the length, *R*, of the monodendron aromatic component. Figure 2b plots both column diameter (*a*, Å) and $T_{\Phi h-i}$ of the ***n*ANfG-4EO-PMA** (**16-*n*-Nf**) series vs the number of methylenic units in the alkyloxy tail, $-(CH_2)_nH$ for ***n*** = 10, 12, 14, and 16. These data show that increasing the alkyloxy tail length results in an increase in the diameter of the column. However, this does not coincide with a significant increase in the stability of the Φ_h LC phase as was observed for the case of aryl methyl ether. For the ***n*ANfG-4EO-PMA** series (***n*** = 10, 12, 14, 16) the column diameter increases on increasing the alkyloxy tail length, but the stability of the Φ_h LC phase reaches a plateau at 152 °C. Notably, the biphenyl derivative **12ABpG-4EO-PMA** (**16-12-Bp**) shows a somewhat different behavior. The length of the (4-(4′-(dodecyloxy)phenyl)benzyl)oxy tail from molecular modeling experiments is 24.9 Å. This value falls between that calculated for the 6-dodecyloxy-2-methylnaphthy-

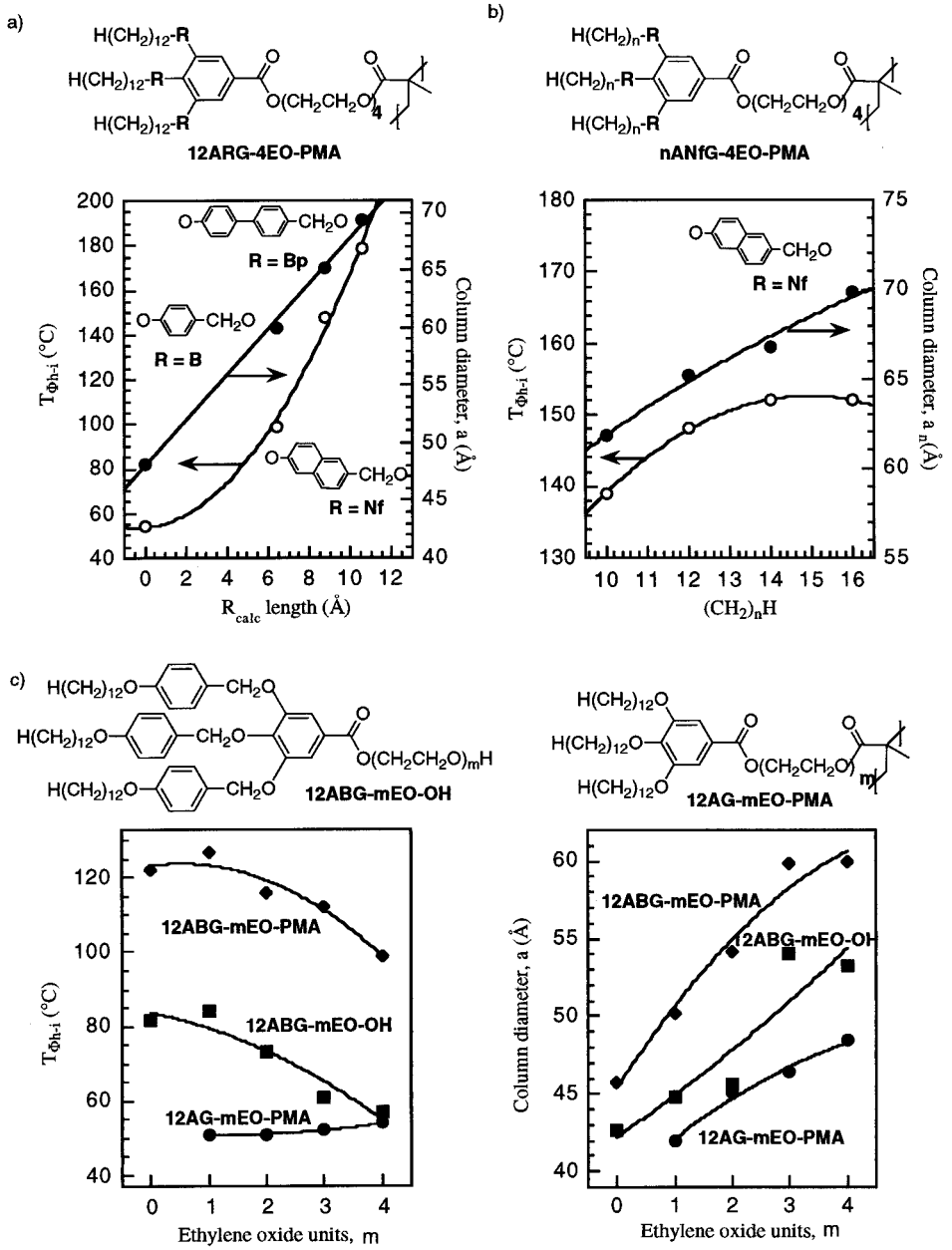

Figure 2. Dependence of isotropization temperature ($T_{\Phi h-i}$, °C) and column diameter (a, Å) of ***n*ANfG-4EO-PMA**, **12ABpG-4EO-PMA**, **12ABG-mEO-PMA**, **12-ABG-mEO-OH**, and **12-AG-mEO-PMA** on (a) aromatic segment length containing the aryl methyl ether part of the monodendron (R_{calc}, Å), (b) alkyloxy tail length, $-(CH_2)_nH$, and (c) number of ethylene oxide units (m).

loxy tail (23.0 Å) and the (6-(tetradecyloxy)naphth-2-yl)methoxy tail (25.6 Å), yet both the diameter and thermal stability of the macromolecular columns generated from the biphenyl monodendrons are distinctly larger than that of the naphthyloxy analogues (Tables 1 and 2). Therefore, a balance exists between the aliphatic sheath and aromatic core, emphasizing the role each plays in the formation of a supramolecular or macromolecular column. While both structural elements are critical for column formation and each contributes to the column breadth, an increase in stability is realized only on increasing the ratio of the aromatic component to the aliphatic tail. Figure 2c plots the dependence of the isotropization temperature ($T_{\Phi h-i}$) on oligooxyethylene spacer length (n) for both the tetraethylene glycol derivatives and the polymethacrylate series. In both cases the thermal stability and structural dimensions are clearly dictated by the aromatic group (R) present in the core of the column. In contrast to increasing the alkyloxy tail length (Figure 2b), increasing the length of the oligooxyethylene spacer results in a decrease in the stability of the Φ_h liquid crystalline phase of **12ABG-*m*EO-PMA** (***m*** = 0−4).[1f] The same trend is observed in the oligooxyethylene monomeric precursor **12ABG-mEO-OH** (***m*** = 1−4), which is most probably a result of accommodating the larger oligooxyethylene tail into the supramolecular structure. The **12AG-*m*EO-PMA** (***m*** = 1−4)[1h] series shows a slight increase in the stability of the Φ_h LC phase. The column diameter increases regularly on increasing the length of the oligooxyethylene spacer, ranging from 45.6 Å[7] for ***m*** = 0 to above 60 Å for ***m*** = 4.[1f] This result matches the trend established by the increase in aliphatic tail length in the ***n*ANfG-4EO-PMA** series (Figure 2b).

The significance of the aromatic component is further emphasized by inspecting a space filling molecular model of the column cross section of **12ANfG-4EO-PMA**

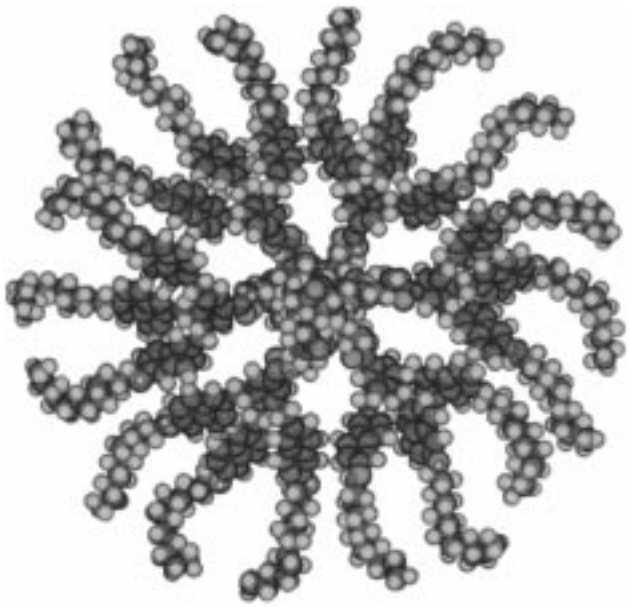

Figure 3. Molecular model of a cross-section of **12ANfG-4EO-PMA** (**16-12-Nf**) in the Φ_h LC phase.

(**16-12-Nf**) in the Φ_h LC phase (Figure 3). The polymethacrylate backbone and oligooxyethylene spacer occupy the column center. The trialkyloxynaphthalene provides structural integrity to the architecture by both π stacking interactions and rigidification of a column layer through decreased conformational freedom. The melted alkyl tails occupy the outermost portion of the column cross-section and compose a region of constant density which is below that of the interior aromatic core. As prescribed by the X-ray data, approximately six taper-shaped monomers occupy a column layer ($\mu = 6.2$, Table 2).

This series of experiments provides access to test the hypothesis of intracolumnar microphase separation between the aromatic core and the aliphatic sheath which was previously proposed for a different self-assembled system.[10] The amphiphilic character of a molecule provides a component of the driving force toward self-assembly, which should be manifested in intramolecular microphase segregation. This model suggests that the supramolecular and macromolecular columns are composed of a core of a fixed width which is surrounded by a sheath of melted alkyl chains of constant density. A detailed discussion of this model for a different class of taper shaped compounds is presented elsewhere.[10] In that case, the model evaluated provided evidence for a microsegregated supramolecular column generated by hydrogen bonding interactions between twin tapered bisamides with different alkyloxy tail lengths by extrapolating to a zero number of methylenic units. Application of this model to the **16-*n*-Nf** series is presented in Figure 4. Extrapolation of a plot of the experimental column diameter squared (a_n^2) vs the number of methylenic units (n) to zero methylenic units (i.e., of the equation $a_n^2 = a_0^2 + Am_H + nAm_{CH_2}$, where n is the number of methylene units, m_H and m_{CH_2} are the respective masses of hydrogen and of methylene units; for more details see ref 10) yields $a_n^2 = a_0^2 + Am_H$ (where A is slope/m_{CH_2}) and thus allows the estimation of the diameter of the aromatic core ($a_n^2 = a_0^2 - Am_H$) in the column ($a_c = a_0$). All experimental data lie within the experimental error of the line fit. This demonstrates that there is little deviation in the density of the aliphatic sheath (ρ_s) over this data range.

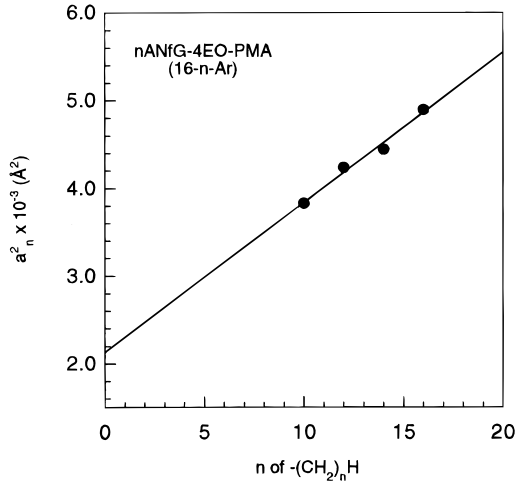

Figure 4. Plot of the square of the column diameter, a^2 (Å^2) vs the number of methylenic units in the alkyl tail, n, of the polymethacrylate series ***n*ANfG-4EO-PMA** (**16-*n*-Nf**).

For the polymethacrylate series ***n*ANfG-4EO-PMA** (**16-*n*-Nf**), the diameter of the aromatic core is $a_c = 46.1$ Å. From the slope of the line (A) the density of the aliphatic sheath (ρ_s) is calculated, $\rho_\sigma = 6\mu/\sqrt{3}dA$ where d is the layer thickness, 3.74 Å[1d,10] This leads to a calculated sheath density of 0.79 g/cm^3 for **12ANfG-4EO-PMA** (**16-12-Nf**) (Table 3), which is larger than the density of liquid n-alkanes (0.75 g/cm^3) yet not as large as that of amorphous polyethylene (0.87 g/cm^3).[10] From ρ_s the corresponding density of the core is calculated, $\rho_c = 1.61$ g/cm^3. This value is significantly larger than ρ_s, and thus it demonstrates the concept of microphase segregation between the core and the aliphatic sheath within these columns. The sheath and core densities calculated from the remaining polymethacrylates follow this trend. Polymethacrylates **10ANfG-4EO-PMA** (**16-10-Nf**) ($\rho_s = 0.78$, $\rho_c = 1.60$ g/cm^3), **14ANfG-4EO-PMA** (**16-14-Nf**) ($\rho_s = 0.77$, $\rho_c = 1.69$ g/cm^3), and **16ANfG-4EO-PMA** (**16-16-Nf**) ($\rho_s = 0.78$, $\rho_c = 1.66$ g/cm^3) (Table 3), all have core densities that are significantly larger than the corresponding sheath densities.

These data were used to calculate the diameter and volume of each element in the composite macromolecular column. From the extrapolation of a^2 vs aliphatic tail length in the polymethacrylate series ***n*ANfG-4EO-PMA** (**16-*n*-Nf**) (Figure 4) to a zero number of methylenic units, the diameter of the core composed of the polymethacrylate backbone, oligooxyethylene spacer, and aromatic segment is $a_c = 46.1$ Å. The density of the aromatic component of the column is extracted from a_c, the formula weight and μ, assuming the density of the combined oligooxyethylene and polymethacrylate ($\rho = 1.228$ g/cm^3 for PMMA).[11] This gives a density for the aromatic component (ρ_{Ar}) of 1.686 g/cm^3. This value is used to calculate the volume of the aromatic component (V_{Ar}) for each polymethacrylate compound in the series, **12AG-4EO-PMA**, **12ABG-4EO-PMA**, and ***n*ANfG-4EO-PMA** (**16-*n*-Ar**) (Table 4). The total volume of a column layer (V_{tot}) is calculated from the column diameter (a) assuming a 3.74 Å layer thickness (i.e., equal to the van der Waals distance). The volume occupied by the oligooxyethylene spacer and polymethacrylate backbone (V_{core}) is considered to remain constant throughout the series. The volume of the aliphatic sheath is obtained by subtracting V_{Ar} and V_{core} from V_{tot}. These values for the ***n*ANfG-4EO-PMA** series compare favorably with the V_s values calculated

Table 3. Characterization of the Microphase Segregation between the Aliphatic Sheath and Aromatic Core in the Macromolecular Columns of *n*ANfG-4EO-PMA (16-*n*-Nf, *n* = 10, 12, 14, 16)

compound	ρ_{exp} (g/cm^3)[a]	μ[b]	$V_s \times 10^{-3}$ (Å^3)[c]	$V_c \times 10^{-3}$ (Å^3)[d]	$V_{tot} \times 10^{-3}$ (Å^3)[e]	ρ_s (g/cm^3)[f]	ρ_c (g/cm^3)[g]
10ANfG-4EO-PMA	1.09	6.2	5.60	5.65	11.25	0.78	1.604
12ANfG-4EO-PMA	1.05	6.3	6.73	5.72	12.45	0.79	1.610
14ANfG-4EO-PMA	1.03	6.1	7.79	5.28	13.07	0.77	1.689
16ANfG-4EO-PMA	1.01	6.2	8.93	5.46	14.39	0.78	1.660

[a] Experimental bulk density (20 °C). [b] Number of tapered monodendrons per column cross section, $\mu = 3\sqrt{3}N_A S^2 d\rho/2M$. [c] Calculated sheath volume, $V_s = [3\mu(n m_{CH_2} + m_H)/N_A]/\rho_s$. [d] Calculated core volume, $V_c = V_{tot} - V_s$. [e] Calculated total volume of a column cross section, $V_{tot} = \pi(a/2)^2 d$. [f] Calculated sheath density, $\rho_s = (6\mu)/\sqrt{3}dA$. [g] Calculated core density, $\rho_c = [\mu(m_c)/N_A]/V_c$.

Table 4. Calculated Diameter and Volume of the Aromatic and Oligooxyethylene/Polymethacrylate Microphase Segregated Components in the Macromolecular Columns of 12AG-4EO-PMA, 12ABG-4EO-PMA, *n*ANfG-4EO-PMA (16-*n*-Nf, *n* = 10, 12, 14, 16) and 12ABpG-4EO-PMA (16-12-Bp)[a]

compound	μ[b]	a (Å)[c]	$V_{tot} \times 10^{-3}$ (Å^3)[d]	$V_s \times 10^{-3}$ (Å^3)[e]	$a_{Ar+core}$ (Å)[f]	$V_{Ar} \times 10^{-3}$ (Å^3)[g]	a_{core} (Å)[h]	$V_{core} \times 10^{-3}$ (Å^3)[i]
12AG-4EO-PMA[j]	4.9	48.4	6.88	3.73 (0.54)	32.7	0.59 (0.08)	29.9	2.62 (0.38)
12ABG-4EO-PMA[k]	5.9	57.2	9.61	4.69 (0.48)	41.0	2.56 (0.26)	29.9	2.62 (0.26)
10ANfG-4EO-PMA	6.2	61.9	11.25	5.60 (0.47)	46.1	3.61 (0.31)	29.9	2.62 (0.22)
12ANfG-4EO-PMA	6.3	65.1	12.45	6.73 (0.52)	46.1	3.67 (0.28)	29.9	2.62 (0.20)
14ANfG-4EO-PMA	6.1	66.7	13.07	7.79 (0.56)	46.1	3.55 (0.25)	29.9	2.62 (0.19)
16ANfG-4EO-PMA	6.2	70.0	14.34	8.93 (0.59)	46.1	3.61 (0.24)	29.9	2.62 (0.17)
12ABpG-4EO-PMA	7.0	69.3	14.11	7.39 (0.51)	47.8	4.48 (0.31)	29.9	2.62 (0.18)

[a] Volume fractions are in parentheses. [b] Number of tapered monodendrons per column cross section, $\mu = 3\sqrt{3}N_A S^2 d\rho/2M$. [c] Column diameter, $a = 2\langle d_{100}\rangle/\sqrt{3}$. [d] Calculated total volume of a column cross section, $V_{tot} = \pi(a/2)^2 d$. [e] Calculated sheath volume, $V_s = V_{tot} - V_{Ar} - V_{core}$. [f] Column diameter of aromatic, oligooxyethylene, and polymethacrylate components. [g] Calculated volume of aromatic component, $V_{Ar} = [\mu(FW)/N_A]/\rho_{Ar}$, where ρ_{Ar} was calculated using the extrapolated core diameter (a_c) and assuming $\rho_{core} = 1.1$ g/mL. [h] Column diameter of oligooxyethylene and polymethacrylate components. [i] Calculated volume of combined oligooxyethylene and polymethacrylate components assuming $\rho_{core} = 1.1$ g/mL. [j] a and μ from ref 1h. [k] a and μ from ref 1f.

in Table 3. The volume of the aromatic ring increases dramatically as we change the structure from 12AG-4EO-PMA (590 Å^3), to **12ABG-4EO-PMA** (2560 Å^3), to **12ANfG-4EO-PMA** (3670 Å^3) and to **12ABpG-4EO-PMA** (4480 Å^3). The volume fraction of each element is also calculated. These results show that in all compounds the aliphatic sheath represents more than 44% of the column and is the dominant volume element in this architecture. The aromatic core occupies between 24 and 31% for the **12ABG-4EO-PMA**, ***n*ANfG-4EO-PMA**, and **12ABpG-4EO-PMA** series and plays a minor role in **12AG-4EO-PMA**, occupying only 8% of the total volume. The volume fractions for the combined oligooxyethylene and polymethacrylate elements range between 17 and 38%.

The contribution of each structural element to the diameter of the macromolecular column is presented in Figure 5. Figure 5a plots the overall diameter of the macromolecular column calculated from X-ray diffraction experiments (a), the diameter of the overal aromatic (i.e., aryl methyl ether and the gallic acid ester), oligooxyethylene and polymethacrylate components ($a_{Ar+core}$), and the diameter of the oligooxyethylene and polymethacrylate core vs the alkyloxy tail length in the ***n*ANfG-4EO-PMA** series (***n*** = 10, 12, 14, 16). As the graph shows, an increase in the alkyloxy tail length leads to a modest increase in the overall column diameter, which ranges from 61.9 to 70.0 Å. In this series, the oligooxyethylene spacer length and aromatic segment remain constant. Figure 5b plots the diameter of the macromolecular column vs the length of the overal aromatic component from molecular modeling experiments. Increasing the size of the aromatic component from a single benzene ring in **12AG-4EO-PMA** to a trisubstituted benzyloxy benzene (**12ABG-4EO-PMA**), to (naphthylmethyl)oxy (**12ANfG-4EO-PMA**), and to (biphenylmethyl)oxy (**12ABpG-4EO-PMA**) results in an increased column diameter due to the increase in the diameter of the aromatic component, ranging from 48.4 to 69.3 Å. In this series the oligooxyethylene component and the length of the aliphatic tail remain constant. Likewise, Figure 5c plots the diameter of the macromolecular column as a function of oligooxyethylene segment length in the **12ABG-*n*EO-PMA** series (***n*** = 0, 1, 2, 3, 4). Again, an increase in the oligooxyethylene segment length leads to an increase in the diameter of the macromolecular column. In this series, the compound without an oligooxyethylene spacer between the polymethacrylate backbone and the taper-shaped building block (**12ABG-PMA**) gives the diameter of the core occupied only by a polymethacrylate backbone (18.3 Å). The manipulation of the oligooxyethylene spacer provides access to macromolecular columns between 45.6 and 60.0 Å.

Figure 5d,e,f schematically shows the microphase segregation model of the column cross-section of each of the polymethacrylates discussed in Figure 5a,b,c, and compares these results to previous results obtained with **12AG-4EO-PMA**[1h] and **12ABG-4EOPMA**.[1f] Figure 5d compares the column cross section of the ***n*ANfG-4EO-PMA** (**16-*n*-Nf**) series (graphically in Figure 5a). Figure 5e shows the column cross sections that result from changing the overall aromatic component in the taper shaped building block, as graphically presented in Figure 5b. Figure 5f shows the five column cross sections from the **12ABG-4EO-PMA** series (graphically in Figure 5c). From inspection of this Figure it is evident that the contribution of the aromatic segment to the column diameter provides the broadest range of

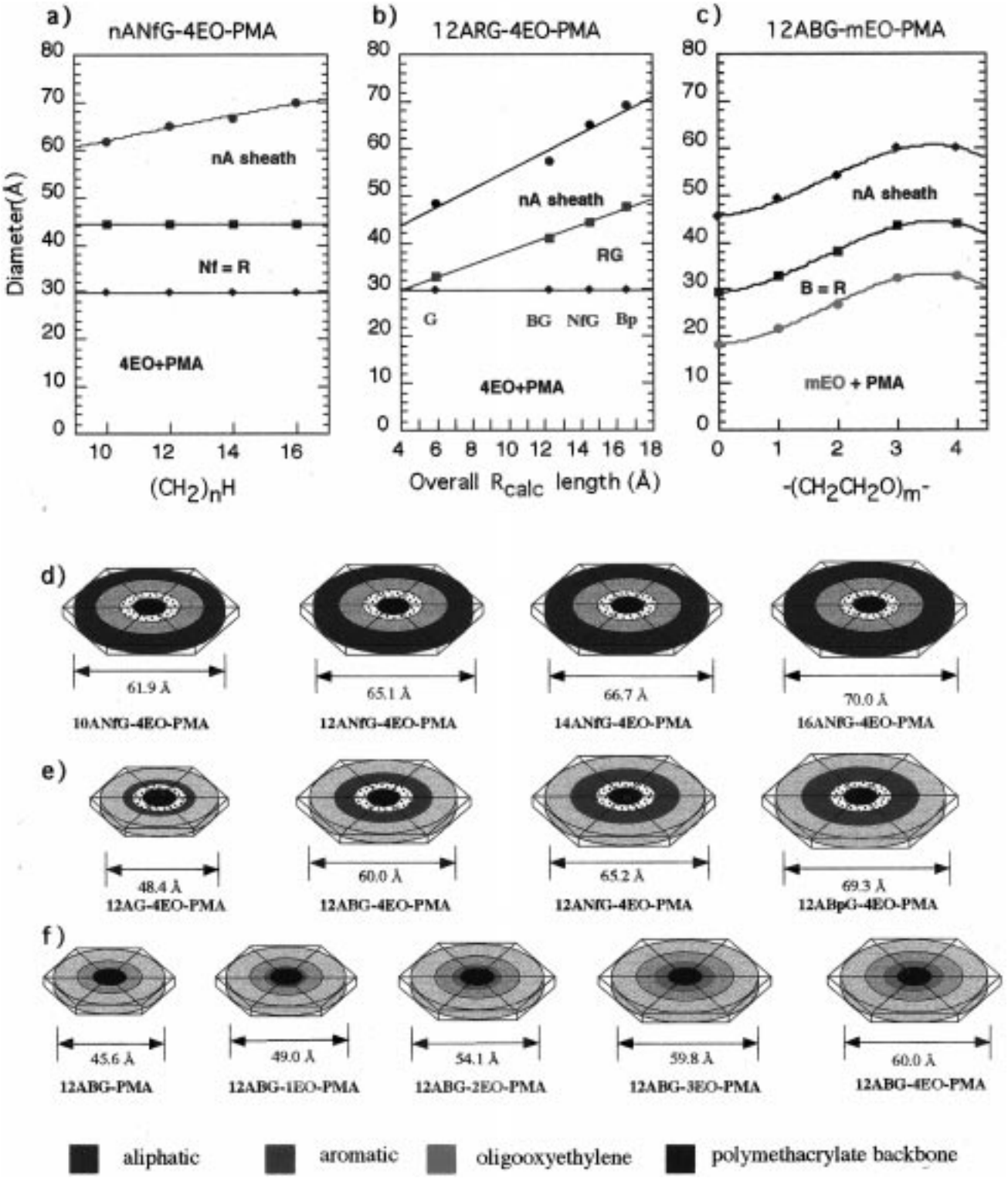

Figure 5. (a−c) Dependence of the macromolecular column (*a*, Å) diameter and the diameter of its constituent microphase segregated components on (a) alkyloxy chain length in the ***n*ANfG-4EO-PMA** (**16-*n*-Nf**, ***n*** = 10, 12, 14, 16) series, (b) overall aromatic group length, which includes the aryl methyl ether and the gallic acid ester (i.e., from molecular modeling for **12AG-4EO-PMA**, **12ABG-4EO-PMA**, **12ANfG-4EO-PMA** (**16-12Nf**), and **12ABpG-4EO-PMA** (**16-12-Bp**), and (c) oligooxyethylene segment length for the **12ABG-*m*EO-PMA** (***m*** = 0, 1, 2, 3, 4) series (column diameter data are recorded at 25 °C (***m*** = 1−4) and 85 °C (***m*** = 0)). (d−f) Schematic representation of a column cross section of polymethacrylates in the Φ_h LC phase: (d) the ***n*ANfG-4EO-PMA** (***n*** = 10, 12, 14, 16) series; (e) **12AG-4EO-PMA**, **12ABG-4EO-PMA**, **12ANfG-4EO-PMA** (**16-12-Nf**), and **12ABpG-4EO-PMA** (**16-12-Bp**); (f) the **12ABG-*m*EO-PMA** (***m*** = 0, 1, 2, 3, 4) series.

column diameters. Furthermore, an increase in the number of methylenic units in the alkyloxy tail (Figure 5d) and length of the oligooxyethylene component (Figure 5f) also leads to an increased column diameter.

Conclusions

These experiments have demonstrated the control the intracolumn superstructure, diameter, and thermal

stability of supramolecular columns self-organized in a Φ_h LC phase by manipulating the aromatic and aliphatic components of their tapered building block generated from first generation AB_3 monodendrons. A systematic change of the aromatic component in all building blocks and in the corresponding polymethacrylates causes an increase in column diameter ranging from 42.6 Å (**8-10-Nf**) to 70.0 Å (**16-16-Nf**). This change also accompanies an increase in the thermal stability of the resulting Φ_h LC phase. This methodology provides a convenient and effective control of the stability and dimensions of a cylindrical supramolecular or macromolecular structure. This strategy is facilitated by the presence of an intracolumnar microphase segregated microstructure. The present data demonstrate the existence of a hydrophilic and aromatic core domain surrounded by an aliphatic sheath of constant density.

Experimental Section

Materials. Methyl 3,4,5-trihydroxybenzoate (98%), 1-bromohexadecane (97%), 1-bromotetradecane (97%), 1-bromododecane (97%), 1-bromodecane (98%), 1,3-dicyclohexylcarbodiimide (DCC, 99%), $LiAlH_4$ (95%), 4-(dimethylamino)pyridine (DMAP, 99%), *p*-toluenesulfonic acid (98%), tetrabutylammonium hydrogen sulfate (TBAH, 97%), HF·pyridine, basic and neutral chromatographic Al_2O_3 (all from Aldrich), *tert*-butyldimethylsilyl chloride (98%, Acros), 6-hydroxy-2-naphthoic acid (Hoechst), chromatographic SiO_2 (Fisher), SiO_2 thin-layer chromatography sheets with fluorescent indicator (Kodak), and other conventional reagents were used as received. Tetraethylene glycol (99%, Aldrich) was stored over 4 Å molecular sieves for more than 24 h and then was vacuum distilled onto 4 Å molecular sieves discarding the forerun. N,N′-Dimethylformamide (DMF) was dried over CaH_2, filtered, and distilled under vacuum. Et_2O was dried over sodium/benzophenone ketyl and distilled. Pyridine and Et_3N were dried over KOH, distilled, and stored over KOH. CH_2Cl_2 and 1,2-dichloroethane were distilled from CaH_2. Methacryloyl chloride (99%, Fluka) was distilled under vacuum from *tert*-butylhydroquinone. Benzene was washed with H_2SO_4 until the washes were colorless and then with water to neutral pH, dried over $MgSO_4$, filtered, and then distilled from sodium/benzophenone ketyl under Ar. 2,2′-Azobisisobutyronitrile (AIBN, Kodak) was recrystallized from MeOH at 4 °C. 4-(Dimethylamino)pyridinium *p*-toluenesulfonate (DPTS) was synthesized as previously described.[1b]

Techniques. ^1H and ^{13}C NMR (200 and 50 MHz respectively) spectra were recorded on a Varian Gemini 200 at 20 °C (unless otherwise noted) with tetramethylsilane (TMS) internal standard. Relative molecular weights of polymers were measured by gel permeation chromatography (GPC) with a Perkin-Elmer Series 10 LC pump equipped with an LC-100 column oven (40 °C), a UV detector, and a Nelson 900 series integrator data station. A set of two Polymer Laboratories PL gel columns of 5×10^2 and 10^4 Å and THF eluent at 1 mL min^{-1} were used. Polystyrene standards were used for calibration. Purities were determined using the same instument in HPLC mode. Melting points were obtained on a Thomas-Hoover capillary melting point apparatus and are uncorrected. IR spectra were recorded on a Perkin-Elmer 1320 spectrometer. Gas chromatagraphy analysis (GC) was perfomed on a Hewlett-Packard 5890 gas chromatograph equipped with a packed column of 10% SP 2100 on 80/100 Supelcoport and a Hewlett-Packard 3392A integrator. Differential scanning calorimetry (DSC) measurements were recorded on a Perkin-Elmer DSC-7. Indium and zinc were used as calibration standards. Heating and cooling rates were 10 °C min^{-1}. First-order transitions are reported as the maximum of endothermic and minimum of exothermic peaks, and glass transitions are recorded as the middle of the change in heat capacity. An Olympus BX40 optical polarized microscope equipped with a Mettler FP82 hot stage and a Mettler FP80 central processor was used to observe thermal transitions and analyze anisotropic textures. Molecular modeling was performed using either CSC Chem3D from Cambridge Scientific Computing, Inc., or MacroModel (Columbia University) on a Silicon Graphics machine. X-ray scattering patterns were recorded using either a helium-filled flat plate wide angle (WAXS) camera or a pinhole-collimated small angle (SAXS) camera, and also by using an image plate area detector (MAR Research) with a graphite monochromatized pinhole-collimated beam and a helium tent. The samples, in glass capillaries, were held in a temperature-controlled cell (±0.1 °C). Ni-filtered Cu Kα radiation was used. Densities (ρ) were determined by floatation in gradient columns. Elemental analysis of all new compounds (M-H-W Laboratories, Phoenix, AZ) agree with the calculated value within less than ±0.4%.

Synthesis of Monomers and Polymers. Ethyl 6-Hydroxy-2-naphthoate (2-Nf). In a 250 mL round-bottom flask containing a Teflon-coated stir bar was placed 15.08 g (0.080 mol) of 6-hydroxy-2-naphthoic acid (**1**), 160 mL of EtOH, and 4 mL of H_2SO_4. The mixture was heated to reflux for 7 h, at which time TLC analysis (1:1 hexanes/ethyl acetate) indicated complete reaction. The reaction mixture was allowed to cool to room temperature, and 100 mL of Et_2O was added. The organic phase was washed once with 200 mL of H_2O and then 100 mL of 5% $NaHCO_3$, 200 mL of H_2O, and 50 mL of saturated NaCl. The organic phase was dried over $MgSO_4$ and then filtered, and the solvent was removed by rotary evaporator to yield 16.2 g (94%) of a white solid. ^1H NMR, δ ($CDCl_3$, TMS, ppm): 1.45 (t, 3H, CH_3, $J = 7.1$), 4.44 (q, 2H, CO_2CH_2, $J = 7.1$), 5.60 (bs, 1H, O*H*), 7.17−7.23 (overlapped m, 2H, H5, H7), 7.67 (d, 1H, H2, $J = 9.0$), 7.83 (d, 1H, H8, $J = 9.7$), 8.01 (dd, 1H, H3, $J_{H3-H4} = 9.0$, $J_{H3-H1} = 1.7$), 8.54 (d, 1H, H1, $J = 1.7$). ^{13}C NMR, δ ($CDCl_3$, TMS, ppm): 14.3 (CH_3), 61.4 (CO_2CH_2), 109.6 (C5), 119.0 (C7), 124.8 (C4′), 125.7 (C4), 126.5 (C8), 127.6 (C8′), 131.2 (C1), 131.4 (C3), 137.3 (C2), 156.3 (C6), 168.0 (*C*=O). IR, ν_{max}(cm^{-1}): 3380 (OH), 1680 (C=O). Mp: 109−110 °C. HPLC: >99%. TLC: $R_f = 0.44$ (1:1 hexanes/ethyl acetate).

Methyl 4-[4′-Hydroxyphenyl]benzoate (2-Bp). Methyl 4-[4′-Hydroxyphenyl]benzoate was synthesized according to a literature procedure.[12] ^1H NMR, δ ($CDCl_3$, TMS, ppm): 3.93 (s, 3H, CO_2CH_3), 4.87 (s, 1H, O*H*), 6.93 (d, 2H, Ar*H ortho* to OH, $J = 8.7$), 7.53 (d, 2H, Ar*H meta* to OH, $J = 8.7$), 7.61 (d, 2H, Ar*H meta* to CO_2CH_3, $J = 8.6$), 8.08 (d, 2H, Ar*H ortho* to CO_2CH_3). Mp: 226−227 °C (lit.[12] mp 227−228 °C).

Ethyl 6-(Dodecyloxy)-2-naphthoate (3-12-Nf). In a 250 mL round-bottom flask with a Teflon-coated magnetic stirring bar was placed 19.7 g (0.077 mol) of 1-bromododecane, 15.8 g (0.073 mol) of ethyl 6-hydroxyethylnaphthoate (**2-Nf**), and 80 mL of DMF. The mixture was sparged with N_2 for 10 min with stirring. K_2CO_3 (25.2 g, 0.183 mol) was crushed and added to the reaction mixture. The reaction was heated to 70 °C and stirred for 13.5 h under a blanket of N_2. ^1H NMR analysis indicated complete reaction. The reaction mixture was allowed to cool to room temperature and then filtered. The filtrate was diluted with 300 mL of Et_2O and then washed once with 200 mL of H_2O, twice with 200 mL of dilute HCl, twice with 200 mL of H_2O, and once with 100 mL of saturated NaCl. The organic phase was dried over $MgSO_4$ and filtered, and the solvent was removed by rotary evaporator. The crude solid was dissolved in a small amount of Et_2O and chromatographed on a short neutral Al_2O_3 column using Et_2O eluent. The resulting product was recrystallized from EtOH, yielding 17.6 g (62%) of white crystals. ^1H NMR, δ ($CDCl_3$, TMS, ppm): 0.88 (t, 3H, CH_3, $J = 6.7$), 1.28 [m, 18H, $(CH_2)_9$], 1.85 (m, 2H, CH_2CH_2OAr), 4.09 (t, 2H, CH_2OAr, $J = 6.4$), 4.42 (q, 2H, $CO_2CH_2CH_3$, $J = 7.1$), 7.10−7.25 (overlapped m, 2H, H5, H7), 7.73 (d, 1H, H4, $J = 8.6$), 7.83 (d, 1H, H8, $J = 8.8$), 8.02 (dd, 1H, H3, $J_{H3-H4} = 8.6$, $J_{H3-H1} = 1.7$), 8.52 (s, 1H, H1). ^{13}C NMR, δ ($CDCl_3$, TMS, ppm): 14.1 (CH_3), 14.3 ($CO_2CH_2CH_3$), 22.6 (CH_3CH_2), 26.0−31.9 [$(CH_2)_9$], 60.7 ($CO_2CH_2CH_3$), 68.0 (CH_2OAr), 106.2 (C5), 119.8 (C7), 125.3 (C4′), 125.8 (C4), 126.6 (C8), 127.7 (C8′), 130.7 (C1,C3), 137.1 (C2), 158.9 (C6), 166.8 (*C*=O). IR, ν_{max} (cm^{-1}): 1710 (C=O). HPLC: >99%. TLC: $R_f = 0.69$ (2:1 hexanes/ethyl acetate). Mp: 51−52 °C.

Ethyl 6-(Decyloxy)-2-naphthoate (3-10-Nf). Ethyl 6-(decyloxy)naphthoate was synthesized according to the procedure described for the synthesis of **3-12-Nf**. From 16.0 g (0.074 mol) **2-Nf** and 17.3 g (0.078 mol) 1-bromodecane was obtained 19.9 g (76%) of white crystals. ^{1}H NMR, δ ($CDCl_3$, TMS, ppm): 0.88 (t, 3H, CH_3, J = 6.7), 1.28 [m, 14H, (CH_2)$_7$], 1.85 (m, 2H, CH_2-CH_2OAr), 4.09 (t, 2H, CH_2OAr, J = 6.4), 4.42 (q, 2H, CO_2CH_2-CH_3, J = 7.1), 7.10−7.25 (overlapped m, 2H, H5, H7), 7.73 (d, 1H, H4, J = 8.6), 7.83 (d, 1H, H8, J = 8.8), 8.02 (dd, 1H, H3, J_{H3-H4} = 8.6, J_{H3-H1} = 1.7), 8.52 (s, 1H, H1). ^{13}C NMR, δ ($CDCl_3$, TMS, ppm): 14.1 (CH_3), 14.3 ($CO_2CH_2CH_3$), 22.6 (CH_3CH_2), 26.0−31.9 [(CH_2)$_7$], 60.7 ($CO_2CH_2CH_3$), 68.0 (CH_2-OAr), 106.2 (C5), 119.8 (C7), 125.3 (C4′), 125.8 (C4), 126.6 (C8), 127.7 (C8′), 130.7 (C1, C3), 137.1 (C2), 158.9 (C6), 166.8 (C=O). IR: ν_{max}(cm^{-1}): 1710 (C=O). HPLC: >99%. TLC: R_f = 0.70 (2:1 hexanes/ethyl acetate). Mp: 44−45 °C.

Ethyl 6-(Tetradecyloxy)-2-naphthoate (3-14-Nf). Compound **3-14-Nf** was synthesized according to the procedure described for the synthesis of **3-12-Nf**. From 12.0 g (0.056 mol) of **2-Nf** and 16.4 g (0.058 mol) of 1-bromotetradecane was obtained 21.1 g (88%) of white crystals. ^{1}H NMR, δ ($CDCl_3$, TMS, ppm): 0.88 (t, 3H, CH_3, J = 6.7), 1.29 [m, 22H, (CH_2)$_{11}$], 1.84 (m, 2H, CH_2CH$_2$OAr), 4.09 (t, 2H, CH_2OAr, J = 6.4), 4.42 (q, 2H, $CO_2CH_2CH_3$, J = 7.1), 7.10−7.25 (overlapped m, 2H, H5, H7), 7.73 (d, 1H, H4, J = 8.6), 7.83 (d, 1H, H8, J = 8.8), 8.02 (dd, 1H, H3, J_{H3-H4} = 8.6, J_{H3-H1} = 1.7), 8.52 (s, 1H, H1). ^{13}C NMR, δ ($CDCl_3$, TMS, ppm): 14.1 (CH_3), 14.3 (CO_2-CH_2CH_3), 22.6 (CH_3CH_2), 26.0−32.0 [(CH_2)$_{11}$], 60.7 (CO_2CH_2-CH_3), 68.1 (CH_2OAr), 106.2 (C5), 119.8 (C7), 125.3 (C4′), 125.8 (C4), 126.6 (C8), 127.7 (C8′), 130.7 (C1, C3), 137.1 (C2), 158.9 (C6), 166.8 (C=O). IR, ν_{max} (cm^{-1}): 1710 (C=O). Mp: 59 °C.

Ethyl 6-(Hexadecyloxy)-2-naphthoate (3-16-Nf). Compound **3-16-Nf** was synthesized according to the procedure described for the synthesis of **3-12-Nf**. From 12.0 g (0.056 mol) of **2-Nf** and 17.8 g (0.058 mol) of 1-bromohexadecane was obtained 20.6 g (84%) of white crystals. ^{1}H NMR, δ ($CDCl_3$, TMS, ppm): 0.88 (t, 3H, CH_3, J = 6.7), 1.29 [m, 26H, (CH_2)$_{13}$], 1.85 (m, 2H, CH_2CH$_2$OAr), 4.09 (t, 2H, CH_2OAr, J = 6.4), 4.42 (q, 2H, $CO_2CH_2CH_3$, J = 7.1), 7.11−7.25 (overlapped m, 2H, H5, H7), 7.73 (d, 1H, H4, J = 8.6), 7.81 (d, 1H, H8, J = 8.8), 8.02 (dd, 1H, H3, J_{H3-H4} = 8.6, J_{H3-H1} = 1.7), 8.52 (s, 1H, H1). ^{13}C NMR, δ ($CDCl_3$, TMS, ppm): 14.1 (CH_3), 14.3 (CO_2-CH_2CH_3), 22.6 (CH_3CH_2), 26.0−32.1 [(CH_2)$_{11}$], 60.7 (CO_2CH_2-CH_3), 68.1 (CH_2OAr), 106.2 (C5), 119.8 (C7), 125.3 (C4′), 125.8 (C4), 126.6 (C8), 127.7 (C8′), 130.7 (C1, C3), 137.2 (C2), 158.9 (C6), 166.8 (C=O). IR, ν_{max} (cm^{-1}): 1710 (C=O). Mp: 64−65 °C.

Methyl 4-[4′-(Dodecyloxy)phenyl]benzoate (3-12-Bp). Methyl 4-[4′-(dodecyloxy)phenyl]benzoate was synthesized according to the procedure described for the synthesis of **3-12-Nf**. From 15.0 g (0.066 mol) of **2-Bp** and 17.4 g (0.070 mol) of 1-bromododecane was obtained 20.7 g (79%) of white flaky crystals. ^{1}H NMR, δ ($CDCl_3$, TMS, ppm): 0.88 (t, 3H, CH_3, J = 7.4), 1.27 [m, 18H, (CH_2)$_9$], 1.86 (m, 2H, CH_2CH$_2$OAr), 3.93 (s, 3H, CO_2CH_3), 4.01 (t, 2H, CH_2OAr, J = 6.4), 6.98 (d, 2H, Ar*H ortho* to CH_2O−, J = 8.8), 7.56 (d, 2H, Ar*H meta* to CH_2O−, J = 8.8), 7.62 (d, 2H, Ar*H meta* to −CO_2CH_3, J = 8.4), 8.08 (d, 2H, Ar*H ortho* to −CO_2CH_3, J = 8.4). ^{13}C NMR, δ ($CDCl_3$, 50 °C, TMS, ppm): 14.0 (CH_3), 22.6 (CH_3CH_2), 26.1−29.6 [(CH_2)$_8$], 31.9 (CH_2CH_2OAr), 51.8 (CO_2CH_3), 68.3 (CH_2-OAr), 115.1 (*ortho* to −OCH_2), 126.4 (*meta* to CO_2CH_3), 128.3 (*meta* to −OCH_2), 130.1 (*ortho* to CO_2CH_3), 132.3 (*ipso* to CO_2-CH_3), 134.1 (*para* to −OCH_2), 145.9 (*para* to CO_2CH_3), 159.6 (*ipso* to −OCH_2), 165.9 (C=O). IR: ν_{max}(cm^{-1}): 1710 (C=O). HPLC: >99%. DSC: first heating, k 123 (14.7), i; second heating, k 122 (14.4), i; cooling, i 117 (2.34), S 113 (1.49), S 96 (10.5), k.

6-(Dodecyloxy)-2-(hydroxymethyl)naphthalene (4-12-Nf). A three-neck 1 L round-bottom flask containing a Teflon-coated magnetic stirring bar was charged with 100 mL of dry Et_2O and 1.9 g (0.05 mol) of $LiAlH_4$. An addition funnel with a N_2 inlet−outlet was placed in the center neck, and the flask was closed with two glass stoppers. Ethyl 6-(dodecyloxy)-2-naphthoate (**3-12-Nf**) (17.4 g, 0.045 mol) was dissolved in 200 mL of dry Et_2O and placed in the addition funnel. The system was flushed with N_2 and attached to a N_2 line. The $LiAlH_4$/Et_2O slurry was then cooled in an ice bath. The Et_2O solution of **3-12-Nf** was added dropwise over a 1.25 h period to the chilled $LiAlH_4$/Et_2O slurry. The reaction mixture was stirred for an additional hour after the addition was complete. ^{1}H NMR indicated complete reaction. H_2O (25 mL) was added to quench the excess $LiAlH_4$; dilute HCl was then added until both phases became transparent. The two phases were separated; the organic one was washed with two 200 mL portions of H_2O and once with 50 mL of saturated NaCl and then dried over $MgSO_4$. The mixture was filtered, and the solvent was removed on a rotary evaporator, resulting in 14.4 g (94%) of white crystals. ^{1}H NMR, δ ($CDCl_3$, TMS, ppm): 0.88 (t, 3H, CH_3, J = 6.7), 1.27 (m, 18H, (CH_2)$_9$], 1.70 (s, 1H, OH), 1.86 (m, 2H, CH_2CH$_2$OAr), 4.07 (t, 2H, CH_2OAr, J = 6.7), 4.81 (s, 2H, CH_2OH), 7.12−7.19 (overlapped m, 2H, H5, H7), 7.44 (dd, 1H, H3, J_{H3-H4} = 8.5, J_{H3-H1} = 1.6), 7.69−7.75 (overlapped m, 3H, H1, H4, H8). ^{13}C NMR, δ ($CDCl_3$, TMS, ppm): 14.1 (CH_3), 22.7 (CH_3CH_2), 26.1−31.9 [(CH_2)$_9$], 65.4 (CH_2OH), 68.1 (CH_2O), 106.5 (C5), 119.3 (C7), 125.5−127.1 (C1, C4, C8), 128.8 (C4′), 129.2 (C3), 134.1 (C2), 135.9 (C8′), 157.2 (C6). IR, ν_{max}(cm^{-1}): 3100−3400 (OH). HPLC: >99%. TLC: R_f = 0.33 (2:1 hexanes/ethyl acetate). Mp: 97−98 °C.

6-(Decyloxy)-2-(hydroxymethyl)naphthalene (4-10-Nf). 6-(Decyloxy)-2-(hydroxymethyl)naphthalene was synthesized according to the procedure described for the synthesis of **4-12-Nf**. From 19.6 g (0.055 mol) of ethyl 6-(decyloxy)ethylnaphthoate (**3-10-Nf**) was obtained 16.0 g (93%) of white flaky crystals. ^{1}H NMR, δ ($CDCl_3$, TMS, ppm): 0.88 (t, 3H, CH_3, J = 6.7), 1.27 (m, 14H, (CH_2)$_7$], 1.70 (s, 1H, OH), 1.86 (m, 2H, CH_2CH$_2$OAr), 4.07 (t, 2H, CH_2OAr, J = 6.7), 4.81 (s, 2H, CH_2-OH), 7.12−7.19 (overlapped m, 2H, H5, H7), 7.44 (dd, 1H, H3, J_{H3-H4} = 8.5, J_{H3-H1} = 1.6), 7.69−7.75 (overlapped m, 3H, H1, H4, H8). ^{13}C NMR, δ ($CDCl_3$, TMS, ppm): 14.1 (CH_3), 22.7 (CH_3CH_2), 26.1−31.9 [(CH_2)$_7$], 65.4 (CH_2OH), 68.1 (CH_2-ONpth), 106.5 (C5), 119.3 (C7), 125.5−127.1 (C1, C4, C8), 128.8 (C4′), 129.2 (C3), 134.1 (C2), 135.9 (C8′), 157.2 (C6). IR, ν_{max}(cm^{-1}): 3100−3400 (OH). HPLC: >99%. TLC: R_f = 0.33 (2:1 hexanes/ethyl acetate). Mp: 93 °C.

6-(Tetradecyloxy)-2-(hydroxymethyl)naphthalene (4-14-Nf). Compound **4-14-Nf** was synthesized according to the procedure described for the synthesis of **4-12-Nf**. From 20.9 g (0.051 mol) of ethyl 6-(tetradecyloxy)ethylnaphthoate (**3-14-Nf**) was obtained 16.0 g (85%) of white flaky crystals. ^{1}H NMR, δ ($CDCl_3$, TMS, ppm): 0.88 (t, 3H, CH_3, J = 6.7), 1.29 (m, 22H, (CH_2)$_{11}$], 1.69 (s, 1H, OH), 1.86 (m, 2H, CH_2CH$_2$OAr), 4.06 (t, 2H, CH_2OAr, J = 6.7), 4.79 (s, 2H, CH_2OH), 7.12−7.20 (overlapped m, 2H, H5, H7), 7.44 (dd, 1H, H3, J_{H3-H4} = 8.5, J_{H3-H1} = 1.6), 7.69−7.75 (overlapped m, 3H, H1, H4, H8). ^{13}C NMR, δ ($CDCl_3$, TMS, ppm): 14.1 (CH_3), 22.7 (CH_3CH_2), 26.1−32.0 [(CH_2)$_{11}$], 65.4 (CH_2OH), 68.1 (CH_2ONpth), 106.5 (C5), 119.3 (C7), 125.5−127.1 (C1, C4, C8), 128.8 (C4′), 129.2 (C3), 134.1 (C2), 135.9 (C8′), 157.2 (C6). IR, ν_{max}(cm^{-1}): 3100−3400 (OH). HPLC: >99%. TLC: R_f = 0.40 (2:1 hexanes/ethyl acetate). Mp: 101−102 °C.

6-(Hexadecyloxy)-2-(hydroxymethyl)naphthalene (4-16-Nf). Compound **4-16-Nf** was synthesized according to the procedure described for the synthesis of **4-12-Nf**. From 20.4 g (0.046 mol) of ethyl 6-(hexadecyloxy)naphthoate (**3-14-Nf**) was obtained 15.0 g (81%) of white flaky crystals. ^{1}H NMR, δ ($CDCl_3$, TMS, ppm): 0.88 (t, 3H, CH_3, J = 6.8), 1.29 (m, 26H, (CH_2)$_{13}$], 1.67 (s, 1H, OH), 1.85 (m, 2H, CH_2CH$_2$OAr), 4.05 (t, 2H, CH_2OAr, J = 6.7), 4.82 (s, 2H, CH_2OH), 7.12−7.19 (overlapped m, 2H, H5, H7), 7.44 (dd, 1H, H3, J_{H3-H4} = 8.5, J_{H3-H1} = 1.6), 7.69−7.75 (overlapped m, 3H, H1, H4, H8). ^{13}C NMR, δ ($CDCl_3$, TMS, ppm): 14.1 (CH_3), 22.7 (CH_3CH_2), 26.1−32.0 [(CH_2)$_{13}$], 65.4 (CH_2OH), 68.1 (CH_2ONpth), 106.5 (C5), 119.3 (C7), 125.5−127.1 (C1, C4, C8), 128.8 (C4′), 129.2 (C3), 134.1 (C2), 135.9 (C8′), 157.2 (C6). IR, ν_{max}(cm^{-1}): 3100−3400 (OH). Mp: 104−105 °C.

4-[4′-(Dodecyloxy)phenyl]benzyl Alcohol (4-12-Bp). 4-[4′-(Dodecyloxy)phenyl]benzyl alcohol was synthesized according to the procedure described for the synthesis of **4-12-Nf**. From 20.6 g (51.8 mmol) of crude material was obtained 14.9 g (78%) of white flaky crystals following recrystallization

from boiling acetone. ^{1}H NMR, δ ($CDCl_3$, TMS, ppm): 0.88 (t, 3H, CH_3, J = 6.9), 1.26 [m, 18H, $(CH_2)_9$], 1.67 (t, 1H, CH_2OH, J = 5.8), 1.80 (m, 2H, CH_2CH_2OAr), 4.00 (t, 2H, CH_2-OAr, J = 6.7), 4.73 (d, 2H, CH_2OH, J = 5.8), 6.96 (d, 2H, Ar*H ortho* to CH_2O-, J = 8.8), 7.41 (d, 2H, Ar*H meta* to $-CH_2OH$, J = 8.4), 7.49−7.58 (overlapped d, 4H, Ar*H meta* to CH_2O-, and Ar*H ortho* to CH_2OH). IR: ν_{max}(cm^{-1}): 3100−3500 (OH). HPLC: >99%. TLC: R_f = 0.28 (2:1 hexanes/ethyl acetate). DSC: first heating, k_1 90 (0.42), k_2 134 (13.7), i; second heating, k_1 90 (0.47), k_2 134 (12.8), i; cooling, i 127 (13.6), k_2 (0.41), k_1 (lit.[13] Mp: 134−135 °C).

6-(Dodecyloxy)-2-(chloromethyl)naphthalene (5-12-Nf). In a 250 mL round-bottom flask containing a Teflon-coated magnetic stirring bar was dissolved 14.25 g (0.042 mol) of **4-12-Nf** in 180 mL of dry CH_2Cl_2 and 1 mL of dry DMF. An addition funnel with N_2 inlet−outlet was attached, and the system was flushed with N_2. $SOCl_2$ (3.5 mL, 0.044 mol) was placed in the addition funnel and added dropwise over 30 min period. The reaction mixture was stirred for an additional 20 min, at which time ^{1}H NMR analysis indicated complete reaction. The solvent was removed on a rotary evaporator and the product was dried under high vacuum resulting in 15.1 g (99%) of white crystals which were used without further purification. ^{1}H NMR, δ ($CDCl_3$, TMS, ppm): 0.88 (t, 3H, CH_3, J = 6.6), 1.27 (m, 18H, $(CH_2)_9$], 1.85 (m, 2H, CH_2CH_2OAr), 4.06 (t, 2H, CH_2OAr, J = 6.6), 4.73 (s, 2H, CH_2Cl), 7.10−7.20 (overlapped m, 2H, H5, H7), 7.45 (dd, 1H, H3, J_{H3-H4} = 8.4, J_{H3-H1} = 1.9), 7.68−7.80 (overlapped m, 3H, H1, H4, H8). ^{13}C NMR, δ ($CDCl_3$, TMS, ppm): 14.1 (CH_3), 22.7 (CH_3CH_2), 26.1−31.9 [$(CH_2)_9$], 46.8 (CH_2Cl), 68.0 (CH_2OAr), 106.4 (C5), 119.5 (C7), 126.7−127.4 (C1, C4, C8), 128.4 (C4′), 129.3 (C3), 132.3 (C2), 134.4 (C8′), 157.6 (C6). IR, ν_{max}(cm^{-1}): 1235, 700 (CH_2-Cl). TLC: R_f = 0.69 (2:1 hexanes/ethyl acetate). Mp: 65 °C.

6-(Decyloxy)-2-(chloromethyl)naphthalene (5-10-Nf). 6-(Decyloxy)-2-(chloromethyl)naphthalene was synthesized according to the procedure described for the synthesis of **5-12-Nf**. From 16.0 g (50.9 mmol) of **4-10-Nf** was obtained 16.9 g (99%) of white flaky crystals. ^{1}H NMR, δ ($CDCl_3$, TMS, ppm): 0.88 (t, 3H, CH_3, J = 6.5), 1.26 (m, 14H, $(CH_2)_7$], 1.86 (m, 2H, CH_2CH_2OAr), 4.06 (t, 2H, CH_2OAr, J = 6.6), 4.73 (s, 2H, CH_2Cl), 7.10−7.20 (overlapped m, 2H, H5, H7), 7.45 (dd, 1H, H3, J_{H3-H4} = 8.4, J_{H3-H1} = 1.9), 7.68−7.80 (overlapped m, 3H, H1, H4, H8). ^{13}C NMR, δ ($CDCl_3$, TMS, ppm): 14.1 (CH_3), 22.7 (CH_3CH_2), 26.1−31.9 [$(CH_2)_7$], 46.8 (CH_2Cl), 68.0 (CH_2-OAr), 106.4 (C5), 119.5 (C7), 126.7−127.4 (C1, C4, C8), 128.4 (C4′), 129.3 (C3), 132.3 (C2), 134.4 (C8′), 157.6 (C6). IR, ν_{max}(cm^{-1}): 1235, 700 (CH_2Cl). TLC: R_f = 0.67 (2:1 hexanes/ethyl acetate). Mp: 57−58 °C.

6-(Tetradecyloxy)-2-(chloromethyl)naphthalene (5-14-Nf). 6-(Tetradecyloxy)-2-(chloromethyl)naphthalene was synthesized according to the procedure described for the synthesis of **5-12-Nf**. From 16.0 g (50.9 mmol) of **4-14-Nf** was obtained 16.8 g (99%) of white flaky crystals. ^{1}H NMR, δ ($CDCl_3$, TMS, ppm): 0.88 (t, 3H, CH_3, J = 6.5), 1.27 (m, 22H, $(CH_2)_{11}$], 1.86 (m, 2H, CH_2CH_2OAr), 4.06 (t, 2H, CH_2OAr, J = 6.6), 4.73 (s, 2H, CH_2Cl), 7.10−7.21 (overlapped m, 2H, H5, H7), 7.45 (dd, 1H, H3, J_{H3-H4} = 8.4, J_{H3-H1} = 1.9), 7.68−7.80 (overlapped m, 3H, H1, H4, H8). ^{13}C NMR, δ ($CDCl_3$, TMS, ppm): 14.1 (CH_3), 22.7 (CH_3CH_2), 26.1−32.0 [$(CH_2)_{11}$], 46.8 (CH_2Cl), 68.0 (CH_2-OAr), 106.4 (C5), 119.5 (C7), 126.7−127.4 (C1, C4, C8), 128.4 (C4′), 129.3 (C3), 132.3 (C2), 134.4 (C8′), 157.6 (C6). IR, ν_{max}(cm^{-1}): 1235, 700 (CH_2Cl). TLC: R_f = 0.69 (2:1 hexanes/ethyl acetate). Mp: 70−71 °C.

6-(Hexadecyloxy)-2-(chloromethyl)naphthalene (5-16-Nf). Compound **5-16-Nf** was synthesized according to the procedure described for the synthesis of **5-12-Nf**. From 11.4 g (28.6 mmol) of **4-16-Nf** was obtained 11.9 g (99%) of white flaky crystals. ^{1}H NMR, δ ($CDCl_3$, TMS, ppm): 0.88 (t, 3H, CH_3, J = 6.7), 1.29 (m, 26H, $(CH_2)_{13}$], 1.85 (m, 2H, CH_2CH_2-OAr), 4.06 (t, 2H, CH_2OAr, J = 6.6), 4.75 (s, 2H, CH_2Cl), 7.10−7.21 (overlapped m, 2H, H5, H7), 7.45 (dd, 1H, H3, J_{H3-H4} = 8.4, J_{H3-H1} = 1.9), 7.68−7.80 (overlapped m, 3H, H1, H4, H8). ^{13}C NMR, δ ($CDCl_3$, TMS, ppm): 14.1 (CH_3), 22.7 (CH_3CH_2), 26.1−32.1 [$(CH_2)_{13}$], 46.8 (CH_2Cl), 68.0 (CH_2OAr), 106.4 (C5), 119.5 (C7), 126.7−127.4 (C1, C4, C8), 128.4 (C4′), 129.3 (C3), 132.3 (C2), 134.4 (C8′), 157.6 (C6). IR, ν_{max}(cm^{-1}): 1235, 700 (CH_2Cl). Mp: 75−76 °C.

4-[4′-(Dodecyloxy)phenyl]benzyl Chloride (5-12-Bp). 4-[4′-(Dodecyloxy)phenyl]benzyl chloride was synthesized according to the procedure described for the synthesis of **5-12-Nf**. From 14.7 g (39.6 mmol) of **4-12-Bp** was obtained 15.2 g (99%) of white crystals of **5-12-Bp**. ^{1}H NMR, δ ($CDCl_3$, TMS, ppm): 0.88 (t, 3H, CH_3, J = 6.8), 1.26 [m, 18H, $(CH_2)_9$], 1.80 (m, 2H, CH_2CH_2OAr), 3.99 (t, 2H, CH_2OAr, J = 6.7), 4.63 (s, 2H, CH_2Cl), 6.96 (d, 2H, Ar*H ortho* to CH_2O-, J = 8.9), 7.42 (d, 2H, Ar*H meta* to $-CH_2Cl$, J = 8.3), 7.49−7.56 (overlapped d, 4H, Ar*H meta* to CH_2O-, and Ar*H ortho* to CH_2Cl). DSC: first heating, k 97 (13.3), i; second heating: k 90, 98 (12.4), i; cooling, i 88, 78 (12.6), k.

Methyl 3,4,5-Tris[(6-(dodecyloxy)naphth-2-yl)methoxy]-benzoate (7-12-Nf). A 500 mL round-bottom flask containing a Teflon-coated magnetic stirring bar was charged with 15.0 g (0.042 mol) of **5-12-Nf**, 2.56 g (0.014 mol) of 3,4,5-trihydroxymethyl benzoate (**6**), and 220 mL of dry DMF. The mixture was sparged with N_2 for 20 min, and then 15.5 g of K_2CO_3 (0.084 mol) was added. N_2 sparging was continued for 10 min further. The reaction mixture was heated to 70 °C for 18.5 h under a blanket of N_2. ^{1}H NMR indicated complete consumption of **5-12-Nf**. The reaction mixture was cooled to room temperature and filtered, and the filtrate was diluted with 300 mL of CH_2Cl_2. The resulting organic phase was washed twice with 200 mL portions of dilute HCl and twice with 200 mL portions of H_2O and then dried over $MgSO_4$. The mixture was filtered, and the solvent was removed using a rotary evaporator. The resulting crude solid was dissolved in CH_2Cl_2 and chromatographed on a short column of neutral Al_2O_3 with CH_2Cl_2 eluent. Recrystallization from acetone yielded 11.1 g (69%) of white crystals. ^{1}H NMR, δ ($CDCl_3$, TMS, ppm): 0.89 (t, 9H, CH_3, J = 7.3), 1.27 (m, 54H, $(CH_2)_9$], 1.86 (m, 6H, CH_2CH_2OAr), 3.89 (s, 3H, CO_2CH_3), 4.08 (m, 6H, CH_2OAr), 5.26 (s, 6H, $ArCH_2OAr$), 6.95−7.18 (overlapped m, 6H, H5, H7), 7.36 (s, 2H, $ArHCO_2CH_3$), 7.40−7.54 [overlapped m, 5H, H3, H1 (*para* to CO_2CH_3), H4 (*para* to CO_2CH_3)], 7.62−7.82 [overlapped m, 7H, H1 (*para* to CO_2CH_3), H4 (*para* to CO_2CH_3), H8]. ^{13}C NMR, δ ($CDCl_3$, TMS, ppm): 14.1 (CH_3), 22.6 (CH_3CH_2), 26.1−31.9 [$(CH_2)_9$], 52.0 (CO_2CH_3), 67.9 (CH_2-OAr), 71.3 ($ArCH_2OAr$, *meta* to CO_2CH_3), 75.3 ($ArCH_2OAr$ *para* to CO_2CH_3), 106.3 (C5), 109.1 (*ortho* to CO_2CH_3), 118.8−119.2 (C7), 125.2 (*ipso* to CO_2CH_3), 125.9−129.4 (C1, C3, C4, C4′, C8), 131.6−132.5 (C2), 134.3 (C8′), 142.5 (*para* to CO_2-CH_3), 152.6 (*meta* to CO_2CH_3), 157.1−157.3 (C6), 166.5 (CO_2-CH_3). IR, ν_{max}(cm^{-1}): 1700 (C═O). TLC: R_f = 0.7 (CH_2Cl_2). Mp: 135−136 °C. HPLC: >99%.

Methyl 3,4,5-Tris[(6-(decyloxy)naphth-2-yl)methoxy-oxy]benzoate (7-10-Nf). Methyl 3,4,5-tris [(6-(decyloxy)-naphth-2-yl)methoxy]methyl benzoate was synthesized according to the procedure described for the synthesis of **7-12-Nf**. From 16.9 g (50.8 mmol) of **5-10-Nf** and 2.92 g (15.9 mmol) of **6** was obtained 14.6 g (86%) of white crystals (after recrystallization from acetone). ^{1}H NMR, δ ($CDCl_3$, TMS, ppm): 0.89 (t, 9H, CH_3, J = 7.3), 1.27 (m, 42H, $(CH_2)_7$], 1.85 (m, 6H, CH_2CH_2OAr), 3.89 (s, 3H, CO_2CH_3), 4.08 (m, 6H, CH_2-OAr), 5.26 (s, 6H, $ArCH_2OAr$), 6.96−7.18 (overlapped m, 6H, H5, H7), 7.36 (s, 2H, $ArHCO_2CH_3$), 7.41−7.54 [overlapped m, 5H, H3, H1 (*para* to CO_2CH_3), H4 (*para* to CO_2CH_3)], 7.62−7.82 [overlapped m, 7H, H1 (*para* to CO_2CH_3), H4 (*para* to CO_2CH_3), H8]. ^{13}C NMR, δ ($CDCl_3$, TMS, ppm): 14.1 (CH_3), 22.6 (CH_3CH_2), 26.1−31.9 [$(CH_2)_7$], 52.0 (CO_2CH_3), 67.9 (CH_2-OAr), 71.3 ($ArCH_2OAr$, *meta* to CO_2CH_3), 75.3 ($ArCH_2OAr$ *para* to CO_2CH_3), 106.3 (C5), 109.1 (*ortho* to CO_2CH_3), 118.8−119.1 (C7), 125.2 (*ipso* to CO_2CH_3), 125.9−129.4 (C1, C3, C4, C4′, C8), 131.6−132.5 (C2), 134.3 (C8′), 142.5 (*para* to CO_2-CH_3), 152.6 (*meta* to CO_2CH_3), 157.1−157.3 (C6), 166.5 (CO_2-CH_3). IR, ν_{max} (cm^{-1}): 1700 (C═O). TLC: R_f = 0.70 (CH_2Cl_2). HPLC: >99%. Mp: 136−137 °C.

Methyl 3,4,5-Tris[(6-(tetradecyloxy)naphth-2-yl)methoxy]benzoate (7-14-Nf). Compound **7-14-Nf** was synthesized according to the procedure described for the synthesis of **7-12-Nf**. From 16.6 g (42.7 mmol) of **5-14-Nf** and 2.45 g (13.3 mmol) of **6** was obtained 14.3 g (87%) of white crystals (after

recrystallization from 2:1 acetone/methyl ethyl ketone). ^{1}H NMR, δ ($CDCl_3$, TMS, ppm): 0.88 (t, 9H, CH_3, J = 7.0), 1.28 (m, 66H, (CH_2)$_{11}$], 1.85 (m, 6H, CH_2CH$_2$OAr), 3.89 (s, 3H, CO_2CH_3), 4.08 (m, 6H, CH_2OAr), 5.27 (s, 6H, ArCH_2OAr), 6.95−7.19 (overlapped m, 6H, H5, H7), 7.37 (s, 2H, ArHCO$_2$-CH$_3$), 7.41−7.55 [overlapped m, 5H, H3, H1 (*para* to CO_2CH_3), H4 (*para* to CO_2CH_3)], 7.62−7.82 [overlapped m, 7H, H1 (*para* to CO_2CH_3), H4 (*para* to CO_2CH_3), H8]. ^{13}C NMR, δ ($CDCl_3$, TMS, ppm): 14.1 (CH_3), 22.6 (CH_3CH_2), 26.0−32.0 [(CH_2)$_{11}$], 52.0 (CO_2CH_3), 67.9 (CH_2OAr), 71.3 (ArCH_2OAr, *meta* to CO_2-CH$_3$), 75.3 (ArCH_2OAr *para* to CO_2CH_3), 106.3 (C5), 109.1 (*ortho* to CO_2CH_3), 118.7−119.1 (C7), 125.2 (*ipso* to CO_2CH_3), 125.9−129.5 (C1, C3, C4, C4′, C8), 131.6−132.5 (C2), 134.3 (C8′), 142.5 (*para* to CO_2CH_3), 152.6 (*meta* to CO_2CH_3), 157.1−157.3 (C6), 166.5 (CO_2CH_3). IR, ν_{max} (cm^{-1}): 1700 (C═O). TLC: R_f = 0.42 (5:1 hexanes/ethyl acetate). HPLC: >99%. Mp: 133−134 °C.

3,4,5-Tris[(6-(hexadecyloxy)naphth-2-yl)methoxy] Benzoate (7-16-Nf). Compound **7-16-Nf** was synthesized according to the procedure described for the synthesis of **7-12-Nf**. From 11.7 g (28.1 mmol) of **5-16-Nf** and 1.62 g (8.79 mmol) of **6** was obtained 7.36 g (63%) of white crystals (after recrystallization from 2:1 acetone/methyl ethyl ketone). ^{1}H NMR, δ ($CDCl_3$, TMS, ppm): 0.88 (t, 9H, CH_3, J = 6.9), 1.28 (m, 78H, (CH_2)$_{13}$], 1.86 (m, 6H, CH_2CH$_2$OAr), 3.89 (s, 3H, CO_2CH_3), 4.08 (m, 6H, CH_2OAr), 5.26 (s, 6H, ArCH_2OAr), 6.95−7.20 (overlapped m, 6H, H5, H7), 7.37 (s, 2H, ArHCO$_2$CH$_3$), 7.41−7.56 [overlapped m, 5H, H3, H1 (*para* to CO_2CH_3), H4 (*para* to CO_2-CH$_3$)], 7.62−7.82 [overlapped m, 7H, H1 (*para* to CO_2CH_3), H4 (*para* to CO_2CH_3), H8]. ^{13}C NMR, δ ($CDCl_3$, TMS, ppm): 14.1 (CH_3), 22.6 (CH_3CH_2), 26.0−32.1 [(CH_2)$_{13}$], 52.0 (CO_2CH_3), 67.9 (CH_2OAr), 71.3 (ArCH_2OAr, *meta* to CO_2CH_3), 75.3 (ArCH_2OAr *para* to CO_2CH_3), 106.3 (C5), 109.1 (*ortho* to CO_2-CH$_3$), 118.7−119.0 (C7), 125.2 (*ipso* to CO_2CH_3), 125.9−129.5 (C1, C3, C4, C4′, C8), 131.6−132.5 (C2), 134.3 (C8′), 142.5 (*para* to CO_2CH_3), 152.6 (*meta* to CO_2CH_3), 157.2−157.3 (C6), 166.5 (CO_2CH_3). IR, ν_{max} (cm^{-1}): 1700 (C═O). TLC: R_f = 0.40 (5:1 hexanes/ethyl acetate). HPLC: >99%. Mp: 134−135 °C.

Methyl 3,4,5-Tris[(4-(4′-(dodecyloxy)phenyl)benzyl)-oxy]benzoate (7-12-Bp). Methyl 3,4,5-tris[(4-(4′-(dodecyloxy)phenyl)benzyl)oxy]benzoate was synthesized according to the procedure described for the synthesis of **7-12-Nf**. From 15.1 g (38.9 mmol) of **5-12-Bp** and 2.31 g (12.6 mmol) of **6** was obtained 7.76 g (50%) of white crystals (after recrystallization from methyl ethyl ketone). ^{1}H NMR, δ ($CDCl_3$, TMS, ppm): 0.88 (t, 9H, CH_3, J = 6.0), 1.27 [m, 54H, (CH_2)$_9$], 1.82 (m, 6H, CH_2CH$_2$OAr), 3.90 (s, 3H, CO_2CH_3), 3.96−4.05 (m, 6H, CH_2-OAr), 5.17 (s, 6H, ArCH_2OAr), 6.89−6.98 (overlapped d, 6H, ArH *ortho* to CH$_2$O−), 7.41−7.57 (overlapped m, 20H, ArH *meta* to −CH$_2$OAr, *meta* to CH$_2$O−, *ortho* to CH$_2$OAr, *ortho* to CO_2CH_3). TLC: R_f = 0.05 (20:1 hexanes/ethyl acetate). Mp: 152−153 °C. HPLC: >99%.

3,4,5-Tris[(6-(dodecyloxy)naphth-2-yl)methoxy]benzoic Acid (8-12-Nf). A 500 mL Erlenmeyer flask containing a Teflon-coated magnetic stirring bar was charged with 10.81 g (9.34 mmol) of **7-12-Nf**, 120 mL of 95% EtOH, and 30 mL of 2-propanol. The mixture was heated to reflux and 3.8 g (68.1 mmol) of solid KOH was added. After 2 h TLC analysis (CH_2-Cl_2) indicated complete reaction. The heterogeneous mixture was cooled to room temperature. The solid was filtered, rinsed with H_2O, and then transferred to a 250 mL Erlenmeyer flask. THF (200 mL) was added, and the mixture was acidified with dilute HCl until pH < 7 was obtained by pH paper. The acidified solution was poured into water and the resulting solid was filtered, then recrystallized from acetone, and dried under high vacuum to yield 10.0 g (94%) of white crystals. ^{1}H NMR, δ ($CDCl_3$, TMS, ppm): 0.88 (t, 9H, CH_3, J = 6.7), 1.27 [m, 54H, (CH_2)$_9$], 1.86 (m, 6H, CH_2CH$_2$OAr), 4.08 (m, 6H, CH_2OAr), 5.27 (s, 6H, ArCH_2OAr), 6.95−7.18 (overlapped m, 6H, H5, H7), 7.37 (s, 2H, ArHCO$_2$H), 7.40−7.54 [overlapped m, 5H, H3, H1 (*para* to CO_2H), H4 (*para* to CO_2H)], 7.62−7.82 [overlapped m, 7H, H1 (*para* to CO_2H), H4 (*para* to CO_2H), H8]. ^{13}C NMR, δ ($CDCl_3$, TMS, ppm): 14.1 (CH_3), 22.7 (CH_3CH_2), 26.1−31.9 [(CH_2)$_9$], 68.0 (CH_2OAr), 71.3 (ArCH_2OAr, *meta* to CO_2H), 75.3 (ArCH_2OAr *para* to CO_2H), 106.3 (C5), 109.5 (*ortho* to CO_2H), 118.8−119.2 (C7), 124.2 (*ipso* to CO_2H), 126.0−129.4 (C1, C3, C4, C4′, C8), 131.5−132.5 (C2), 134.3 (C8′), 143.2 (*para* to CO_2H), 152.6 (*meta* to CO_2H), 157.1−157.3 (C6), 171.6 (CO_2H). IR, ν_{max}(cm^{-1}): 1680 (C═O). HPLC: >99%. TLC: R_f = 0 (CH_2Cl_2). Thermal transitions and corresponding enthalpy changes are recorded in Table 4.1.

3,4,5-Tris[(6-(decyloxy)naphth-2-yl)methoxy]benzoic Acid (8-10-Nf). 3,4,5-Tris[(6-(decyloxy)naphth-2-yl)methoxy]-benzoic acid was synthesized according to the procedure described for the synthesis of **8-12-Nf**. From 14.1 g (13.0 mmol) of **7-10-Nf** was obtained 13.1 g (95%) of a white solid. ^{1}H NMR, δ ($CDCl_3$, TMS, ppm): 0.88 (t, 9H, CH_3, J = 6.8), 1.26 [m, 42H, (CH_2)$_7$], 1.86 (m, 6H, CH_2CH$_2$OAr), 4.07 (m, 6H, CH_2OAr), 5.27 (s, 6H, ArCH_2OAr), 6.94−7.19 (overlapped m, 6H, H5, H7), 7.37 (s, 2H, ArHCO$_2$H), 7.40−7.54 [overlapped m, 5H, H3, H1 (*para* to CO_2H), H4 (*para* to CO_2H)], 7.62−7.82 [overlapped m, 7H, H1 (*para* to CO_2H), H4 (*para* to CO_2H), H8]. ^{13}C NMR, δ ($CDCl_3$, TMS, ppm): 14.1 (CH_3), 22.7 (CH_3CH_2), 26.0−31.9 [(CH_2)$_7$], 68.0 (CH_2ONpth), 71.2 (NpthCH_2-OAr, *meta* to CO_2H), 75.3 (NpthCH_2OAr *para* to CO_2H), 106.3 (C5), 109.5 (*ortho* to CO_2H), 118.8−119.2 (C7), 124.2 (*ipso* to CO_2H), 126.0−129.5 (C1, C3, C4, C4′, C8), 131.5−132.5 (C2), 134.3 (C8′), 143.1 (*para* to CO_2H), 152.6 (*meta* to CO_2H), 157.1−157.2 (C6), 171.6 (CO_2H). IR, ν_{max}(cm^{-1}): 1680 (C═O). HPLC: >99%. TLC: R_f = 0 (CH_2Cl_2). Thermal transitions and corresponding enthalpy changes are recorded in Table 4.1.

3,4,5-Tris[6-(tetradecyloxy)naphth-2-yl)methoxy]benzoic Acid (8-14-Nf). Compound **8-14-Nf** was synthesized according to the procedure described for the synthesis of **8-12-Nf**. From 6.08 g (4.83 mmol) of **7-14-Nf** was obtained 5.26 g (89%) of a white solid. ^{1}H NMR, δ ($CDCl_3$, TMS, ppm): 0.88 (t, 9H, CH_3, J = 6.9), 1.26 [m, 66H, (CH_2)$_{11}$], 1.86 (m, 6H, CH_2-CH$_2$OAr), 4.07 (m, 6H, CH_2OAr), 5.26 (s, 6H, ArCH_2OAr), 6.94−7.20 (overlapped m, 6H, H5, H7), 7.37 (s, 2H, ArHCO$_2$H), 7.40−7.54 [overlapped m, 5H, H3, H1 (*para* to CO_2H), H4 (*para* to CO_2H)], 7.62−7.82 [overlapped m, 7H, H1 (*para* to CO_2H), H4 (*para* to CO_2H), H8]. ^{13}C NMR, δ ($CDCl_3$, TMS, ppm): 14.1 (CH_3), 22.7 (CH_3CH_2), 26.0−32.1 [(CH_2)$_{11}$], 68.1 (CH_2ONpth), 71.2 (NpthCH_2OAr, *meta* to CO_2H), 75.3 (NpthCH_2OAr *para* to CO_2H), 106.3 (C5), 109.5 (*ortho* to CO_2H), 118.8−119.2 (C7), 124.2 (*ipso* to CO_2H), 126.1−129.7 (C1, C3, C4, C4′, C8), 131.5−132.4 (C2), 134.3 (C8′), 143.1 (*para* to CO_2H), 152.6 (*meta* to CO_2H), 157.1−157.2 (C6), 171.6 (CO_2H). IR, ν_{max}-(cm^{-1}): 1680 (C═O). HPLC: >99%. TLC: R_f = 0 (CH_2Cl_2). Thermal transitions and corresponding enthalpy changes are recorded in Table 4.1.

3,4,5-Tris[(6-(hexadecyloxy)naphth-2-yl)methoxy]benzoic Acid (8-16-Nf). Compound **8-16-Nf** was synthesized according to the procedure described for the synthesis of **8-12-Nf**. From 3.02 g (2.26 mmol) of **7-14-Nf** was obtained 2.40 g (81%) of a white solid. ^{1}H NMR, δ ($CDCl_3$, TMS, ppm): 0.88 (t, 9H, CH_3, J = 6.7), 1.26 [m, 78H, (CH_2)$_{13}$], 1.86 (m, 6H, CH_2-CH$_2$OAr), 4.06 (m, 6H, CH_2OAr), 5.26 (s, 6H, ArCH_2OAr), 6.93−7.19 (overlapped m, 6H, H5, H7), 7.37 (s, 2H, ArHCO$_2$H), 7.40−7.54 [overlapped m, 5H, H3, H1 (*para* to CO_2H), H4 (*para* to CO_2H)], 7.63−7.82 [overlapped m, 7H, H1 (*para* to CO_2H), H4 (*para* to CO_2H), H8]. ^{13}C NMR, δ ($CDCl_3$, TMS, ppm): 14.1 (CH_3), 22.7 (CH_3CH_2), 26.0−32.1 [(CH_2)$_{13}$], 68.1 (CH_2ONpth), 71.2 (NpthCH_2OAr, *meta* to CO_2H), 75.3 (NpthCH_2OAr *para* to CO_2H), 106.3 (C5), 109.5 (*ortho* to CO_2H), 118.8−119.2 (C7), 124.2 (*ipso* to CO_2H), 126.0−129.7 (C1, C3, C4, C4′, C8), 131.5−132.4 (C2), 134.3 (C8′), 143.1 (*para* to CO_2H), 152.6 (*meta* to CO_2H), 157.1−157.2 (C6), 171.6 (CO_2H). IR ν_{max}-(cm^{-1}): 1680 (C═O). HPLC: >99%. TLC: R_f = 0 (CH_2Cl_2). Thermal transitions and corresponding enthalpy changes are recorded in Table 4.1.

3,4,5-Tris[(4-(4′-(dodecyloxy)phenyl)benzyl)oxy]benzoic Acid (8-12-Bp). 3,4,5-Tris[(4-(4′-(dodecyloxy)phenyl)-benzyl)oxy]benzoic acid was hydrolyzed using a modified procedure. A 500 mL flask containing a Teflon-coated magnetic stirring bar was charged with 7.66 g (6.18 mmol) of **7-12-Bp**, 3.0 g of KOH, 0.9 g of TBAH, and 200 mL of 2-propanol. The reaction mixture was heated to reflux for 1.5 h, at which time ^{1}H NMR indicated complete hydrolysis. The reaction mixture was cooled to room temperature and filtered. The

filtered solid was transferred to a 500 mL Erlenmeyer flask, and 200 mL of THF was added. Dilute HCl was added dropwise to the mixture until pH < 7 was obtained. The product was precipitated into 400 mL of H_2O, then filtered and rinsed with H_2O. The product was recrystallized from methyl ethyl ketone to yield 5.78 g (76%) of white crystals. ^{1}H NMR, δ ($CDCl_3$, TMS, ppm): 0.88 (t, 9H, CH_3, J = 7.1), 1.27 [m, 54H, (CH_2)$_9$], 1.86 (m, 6H, CH_2CH$_2$OAr), 3.99−4.05 (m, 6H, CH_2OAr), 5.18 (s, 6H, ArCH_2OAr), 6.89−6.97 (overlapped d, 6H, Ar*H ortho* to CH_2O−), 7.42−7.57 (overlapped m, 20H, Ar*H meta* to −CH_2OAr, *meta* to CH_2O−, *ortho* to CH_2OAr, *ortho* to CO_2H). ^{13}C NMR, δ ($CDCl_3$, 45 °C, TMS, ppm): 14.1 (*C*H$_3$), 22.7 (CH$_3$*C*H$_2$), 26.1−29.6 [(*C*H$_2$)$_8$], 32.0 (*C*H$_2$CH$_2$Ar), 68.3 (*C*H$_2$OAr), 71.3 (Ar*C*H$_2$OAr, *meta* to CO_2H), 75.2 (Ar*C*H$_2$-OAr *para* to CO_2H), 110.1 (*ortho* to CO_2H), 115.0 (*ortho* to −OCH$_2$CH$_2$ on the biphenyl), 124.3 (*ipso* to CO_2H), 126.5−126.8 (*meta* to −CH_2OAr on the biphenyl), 128.1−129.0 (*ortho* to −CH_2OAr on the biphenyl, *meta* to −OCH$_2$CH$_2$ on the biphenyl), 133.2 (*ipso* to −CH_2OAr on the biphenyl), 135.0−135.9 (*para* to −OCH$_2$CH$_2$ on the biphenyl, *para* to −CH_2OAr on the biphenyl), 140.8 (*para* to CO_2H), 152.8 (*meta* to CO_2H), 159.0 (*ipso* to −OCH$_2$CH$_2$ on the biphenyl), 170.8 (C═O). IR: ν_{max}(cm^{-1}): 1690 (C═O).TLC: R_f = 0 (CH_2Cl_2). HPLC: >99%. Thermal transitions and corresponding enthalpy changes are listed in Table 4.1.

2-{2-(2-(2-(*tert*-Butyldimethylsiloxy)ethoxy)ethoxy]-ethoxy}ethanol (11). The monoprotection of tetraethylene glycol to yield **11** was perfomed following a modified literature procedure.[7] A 100 mL round-bottom flask containing a Teflon-coated magnetic stirring bar was charged with 3.45 g (0.023 mol) of *tert*-butyldimethylsilyl chloride (**10**), 10 mL of DMF, 50.3 g (0.26 mol) of tetraethylene glycol (**9**), 4 mL (0.026 mol) of Et_3N, and 0.12 g (0.9 mmol) of DMAP. The flask was flushed with N_2 and stirred for 1.5 h under a N_2 atmosphere. ^{1}H NMR indicated complete consumption of **10**. The reaction mixture was poured into 300 mL of $CHCl_3$ and extracted three times with 200 mL portions of H_2O and then once with 100 mL of saturated NH_4Cl. The organic was dried over Na_2SO_4 and filtered, and the solvent was removed using a rotary evaporator. The crude product was then dissolved in Et_2O and washed twice with 100 mL of H_2O, then with 50 mL of saturated NaCl. The solution was dried over Na_2SO_4 and filtered, and the solvent was removed using a rotary evaporator. The product was dried under high vacuum to yield 6.6 g (92%) of a colorless liquid. GC: 92.2% monoprotected; 7.8% diprotected. ^{1}H NMR, δ ($CDCl_3$, TMS, ppm): 0.06 [s, 6H, OSi-(CH_3)$_2$], 0.89 (s, 9H, C(CH_3)$_3$], 3.55−3.80 [overlapped m, 16H, (CH_2CH_2O)$_4$H]. ^{13}C NMR, δ ($CDCl_3$, TMS, ppm): −5.4 [OSi-(*C*H$_3$)$_2$], 18.2 [*C*(CH$_3$)$_3$], 25.8 [C(*C*H$_3$)$_3$], 61.5 (*C*H$_2$OH), 62.6 (*C*H$_2$OSi(CH$_3$)$_2$], 70.2−72.5 [*C*H$_2$(O*C*H$_2$*C*H$_2$)$_2$O*C*H$_2$]. IR, ν_{max}(cm^{-1}): 3100−3600 (OH), 1250, 1100 (SiOCH$_2$).

2-{2-[2-(2-(*tert*-Butyldimethylsiloxyethoxy)ethoxy]-ethoxy}ethyl 3,4,5-Tris((6-(dodecyloxy)lnaphth-2-yl)-methoxy)benzoate (12-12-Nf). A 100 mL round-bottom flask containing a Teflon-coated magnetic stirring bar was flushed with N_2 and charged with 2.01 g (1.75 mmol) of **8-12-Nf**, 0.66 g (2.1 mmol) of 2-{2-[2-(2-*tert*-butyl dimethyl-siloxyethoxy)ethoxy]ethoxy}ethanol (**11**), 30 mL of dry CH_2-Cl_2, 0.073 g (0.35 mmol) of DPTS, and 0.43 g (2.1 mmol) DCC. The reaction mixture was heated to reflux for 15.5 h under N_2. ^{1}H NMR indicated complete reaction. The reaction mixture was filtered, and the filtrate was concentrated until a precipitate was evident. CH_2Cl_2 was added to disperse the solids, and the mixture was filtered again. The filtrate solvent was removed using a rotary evaporator, and the crude product was chromatographed on neutral Al_2O_3 using 2:1 hexanes/ethyl acetate eluent, yielding 1.6 g (64%) of a white solid. ^{1}H NMR, δ ($CDCl_3$, TMS, ppm): 0.04 [s, 6H, OSi(CH_3)$_2$], 0.88 (overlapped m, 18H, CH_3, OSi(CH$_2$)$_2$C(CH_3)$_3$], 1.27 [m, 54H, (CH_2)$_9$], 1.86 (m, 6H, CH_2CH$_2$OAr), 3.52 (t, 2H, CH_2OSi, J = 5.5), 3.63−3.82 [m, 12H, CH_2O(CH_2CH_2O)$_2$CH_2], 4.08 (m, 6H, CH_2OAr), 4.45 (t, 2H, CO_2C*H*$_2$, J = 5.4), 5.26 (s, 6H, ArCH_2OAr), 6.99−7.17 (overlapped m, 6H, H5, H7), 7.35 (s, 2H, Ar*H*CO$_2$CH$_2$), 7.40−7.53 [overlapped m, 5H, H3, H1 (*para* to CO$_2$CH$_2$), H4 (*para* to CO$_2$CH$_2$)], 7.62−7.82 [overlapped m, 7H, H1 (*para* to CO$_2$CH$_2$), H4 (*para* to CO$_2$CH$_2$), H8]. ^{13}C NMR, δ ($CDCl_3$, TMS, ppm): −5.3 [Si(*C*H$_3$)$_2$], 14.1 (*C*H$_3$), 18.2 [*C*(CH$_3$)$_3$], 22.7 (CH$_3$*C*H$_2$), 25.9−31.9 [(*C*H$_2$)$_9$], 62.7 (*C*H$_2$OSi), 64.2 (CO_2CH$_2$), 68.0 (*C*H$_2$OAr), 69.2−70.7, 72.6 [CH$_2$(OCH$_2$CH$_2$)$_2$OCH$_2$], 71.5 (Ar*C*H$_2$OAr, *meta* to CO$_2$CH$_2$), 75.3 (Ar*C*H$_2$OAr *para* to CO$_2$-CH$_2$), 106.3−106.4 (C5), 109.4 (*ortho* to CO$_2$CH$_2$), 118.9−119.3 (C7), 125.2 (*ipso* to CO$_2$CH$_2$), 126.0−129.4 (C1, C3, C4, C4′, C8), 131.7−132.5 (C2), 134.3 (C8′), 142.7 (*para* to CO$_2$CH$_2$), 152.6 (*meta* to CO$_2$CH$_2$), 157.4 (C6), 165.6 (*C*O$_2$CH$_2$). IR, ν_{max}(cm^{-1}): 1710 (C═O), 1205, 1100 (SiOCH$_2$). HPLC: >99%. Mp: 56−57 °C. TLC: R_f = 0.44 (2:1 hexanes/ethyl acetate).

2-{2-[2-(2-(*tert*-Butyldimethylsiloxy)ethoxy)ethoxy]-ethoxy}ethyl 3,4,5-Tris((6-(decyloxy)-2-naphth-2-yl)-methoxy)benzoate (12-10-Nf). 2-{2-[2-(2-(*tert*-Butyldime-thylsiloxy)ethoxy)ethoxy]ethoxy}ethyl 3,4,5-tris((6-(decyloxy)-naphth-2-yl)methoxy)benzoate was synthesized according to the procedure described for the synthesis of **12-12-Nf**. From 1.00 g (0.943 mmol) of **8-10-Nf** and 0.350 g (1.13 mmol) of **11** was obtained 0.76 g (60%) of a white solid following column chromatography (neutral Al_2O_3, 3:1 hexanes/ethyl acetate). ^{1}H NMR, δ ($CDCl_3$, TMS, ppm): 0.04 [s, 6H, OSi(CH_3)$_2$], 0.88 (overlapped m, 18H, CH_3, OSi(CH$_2$)$_2$C(CH_3)$_3$], 1.26 [m, 42H, (CH_2)$_7$], 1.86 (m, 6H, CH_2CH$_2$OAr), 3.52 (t, 2H, CH_2OSi, J = 5.5), 3.61−3.82 [m, 12H, CH_2O(CH_2CH_2O)$_2$CH_2], 4.08 (m, 6H, CH_2OAr), 4.44 (t, 2H, CO_2C*H*$_2$, J = 5.4), 5.26 (s, 6H, ArCH_2-OAr), 6.99−7.17 (overlapped m, 6H, H5, H7), 7.34 (s, 2H, Ar*H*CO$_2$CH$_2$), 7.40−7.53 [overlapped m, 5H, H3, H1 (*para* to CO$_2$CH$_2$), H4 (*para* to CO$_2$CH$_2$)], 7.63−7.82 [overlapped m, 7H, H1 (*para* to CO$_2$CH$_2$), H4 (*para* to CO$_2$CH$_2$), H8]. ^{13}C NMR, δ ($CDCl_3$, TMS, ppm): −5.3 [Si(*C*H$_3$)$_2$], 14.1 (*C*H$_3$), 18.2 [*C*(CH$_3$)$_3$], 22.7 (CH$_3$*C*H$_2$), 25.9−31.9 [(*C*H$_2$)$_7$], 62.7 (*C*H$_2$OSi), 64.2 (CO_2CH$_2$), 68.0 (*C*H$_2$ONpth), 69.2−70.7, 72.6 [CH$_2$(O*C*H$_2$-*C*H$_2$)$_2$O*C*H$_2$], 71.5 (NpthCH$_2$OAr, *meta* to CO$_2$CH$_2$), 75.3 (NpthCH$_2$OAr *para* to CO$_2$CH$_2$), 106.3−106.4 (C5), 109.4 (*ortho* to CO$_2$CH$_2$), 118.9−119.4 (C7), 125.2 (*ipso* to CO$_2$CH$_2$), 126.0−129.4 (C1, C3, C4, C4′, C8), 131.8−132.5 (C2), 134.3 (C8′), 142.7 (*para* to CO$_2$CH$_2$), 152.6 (*meta* to CO$_2$CH$_2$), 157.4 (C6), 165.6 (CO$_2$CH$_2$). IR, ν_{max}(cm^{-1}): 1710 (C═O), 1205, 1100 (SiOCH$_2$). HPLC: >99%. Mp: 57−58 °C. TLC: R_f = 0.36 (2:1 hexanes/ethyl acetate).

2-{2-[2-(2-(*tert*-Butyldimethylsiloxy)ethoxy)ethoxy]-ethoxy}ethyl 3,4,5-(Tris((6-(tetradecyloxy)naphth-2-yl)-methoxy)benzoate (12-14-Nf). Compound **12-14-Nf** was synthesized according to the procedure described for the synthesis of **12-12-Nf**. From 3.00 g (2.44 mmol) of **8-10-Nf** and 0.904 g (2.93 mmol) of **11** was obtained 2.45 g (66%) of a white solid following column chromatography (SiO_2, 2:1 hexanes/ethyl acetate). ^{1}H NMR, δ ($CDCl_3$, TMS, ppm): 0.04 [s, 6H, OSi(CH_3)$_2$], 0.89 (overlapped m, 18H, CH_3, OSi(CH$_2$)$_2$C-(CH_3)$_3$], 1.26 [m, 66H, (CH_2)$_{11}$], 1.86 (m, 6H, CH_2CH$_2$OAr), 3.52 (t, 2H, CH_2OSi, J = 5.5), 3.61−3.83 [m, 12H, CH_2O-(CH_2CH_2O)$_2$CH_2], 4.08 (m, 6H, CH_2OAr), 4.43 (t, 2H, CO_2C*H*$_2$, J = 5.4), 5.26 (s, 6H, ArCH_2OAr), 6.99−7.17 (overlapped m, 6H, H5, H7), 7.34 (s, 2H, Ar*H*CO$_2$CH$_2$), 7.40−7.53 [overlapped m, 5H, H3, H1 (*para* to CO$_2$CH$_2$), H4 (*para* to CO$_2$CH$_2$)], 7.63−7.83 [overlapped m, 7H, H1 (*para* to CO$_2$CH$_2$), H4 (*para* to CO$_2$CH$_2$), H8]. ^{13}C NMR, δ ($CDCl_3$, TMS, ppm): −5.3 [Si-(*C*H$_3$)$_2$], 14.1 (*C*H$_3$), 18.2 [*C*(CH$_3$)$_3$], 22.7 (CH$_3$*C*H$_2$), 25.8−31.9 [(*C*H$_2$)$_{11}$], 62.7 (*C*H$_2$OSi), 64.2 (CO_2CH$_2$), 68.0 (*C*H$_2$ONpth), 69.2−70.8, 72.6 [CH$_2$(O*C*H$_2$*C*H$_2$)$_2$O*C*H$_2$], 71.5 (NpthCH$_2$OAr, *meta* to CO$_2$CH$_2$), 75.3 (NpthCH$_2$OAr *para* to CO$_2$CH$_2$), 106.3−106.4 (C5), 109.4 (*ortho* to CO$_2$CH$_2$), 119.0−119.4 (C7), 125.2 (*ipso* to CO$_2$CH$_2$), 126.0−129.4 (C1, C3, C4, C4′, C8), 131.8−132.5 (C2), 134.3 (C8′), 142.7 (*para* to CO$_2$CH$_2$), 152.6 (*meta* to CO$_2$CH$_2$), 157.4 (C6), 165.6 (CO$_2$CH$_2$). HPLC: >99%. Mp: 60−61 °C.

2-{2-[2-(2-(*tert*-Butyldimethylsiloxy)ethoxy)ethoxy]-ethoxy}ethyl 3,4,5-Tris((6-(hexadecyloxy)naphth-2-yl)-methoxy)benzoate (12-16-Nf). Compound **12-16-Nf** was synthesized according to the procedure described for the synthesis of **12-12-Nf** using 5:1 CH_2Cl_2/DCE as solvent. From 2.10 g (1.60 mmol) of **8-16-Nf** and 0.592 g (1.92 mmol) of **11** was obtained 1.99 g (78%) of a white solid following column chromatography (SiO_2, 2:1 hexanes/ethyl acetate). ^{1}H NMR, δ ($CDCl_3$, TMS, ppm): 0.04 [s, 6H, OSi(CH_3)$_2$], 0.89 (overlapped

m, 18H, CH_3, OSi(CH$_2$)$_2$C(CH_3)$_3$], 1.26 [m, 78H, (CH_2)$_{13}$], 1.85 (m, 6H, CH_2CH$_2$OAr), 3.52 (t, 2H, CH_2OSi, J = 5.4), 3.61−3.83 [m, 12H, CH_2O(CH_2CH_2O)$_2$CH_2], 4.08 (m, 6H, CH_2OAr), 4.43 (t, 2H, CO$_2$CH_2, J = 5.4), 5.26 (s, 6H, ArCH_2OAr), 7.00−7.19 (overlapped m, 6H, H5, H7), 7.34 (s, 2H, ArHCO$_2$CH$_2$), 7.40−7.55 [overlapped m, 5H, H3, H1 (*para* to CO$_2$CH$_2$), H4 (*para* to CO$_2$CH$_2$)], 7.62−7.83 [overlapped m, 7H, H1 (*para* to CO$_2$CH$_2$), H4 (*para* to CO$_2$CH$_2$), H8]. ^{13}C NMR, δ (CDCl$_3$, TMS, ppm): −5.3 [Si(CH$_3$)$_2$], 14.1 (*C*H$_3$), 18.2 [*C*(CH$_3$)$_3$], 22.7 (CH$_3$*C*H$_2$), 25.9−32.0 [(*C*H$_2$)$_{11}$], 62.7 (*C*H$_2$OSi), 64.2 (CO$_2$*C*H$_2$), 68.0 (*C*H$_2$ONpth), 69.2−70.8, 72.6 [*C*H$_2$(OC*H*$_2$*C*H$_2$)$_2$OC*H*$_2$], 71.5 (NpthC*H*$_2$OAr, *meta* to CO$_2$CH$_2$), 75.3 (NpthC*H*$_2$OAr *para* to CO$_2$CH$_2$), 106.3−106.5 (C5), 109.4 (*ortho* to CO$_2$CH$_2$), 119.0−119.4 (C7), 125.2 (*ipso* to CO$_2$CH$_2$), 126.0−129.4 (C1, C3, C4, C4′, C8), 131.8−132.5 (C2), 134.3 (C8′), 142.7 (*para* to CO$_2$CH$_2$), 152.6 (*meta* to CO$_2$CH$_2$), 157.4 (C6), 165.6 (*C*O$_2$CH$_2$). HPLC: >99%. Mp: 64−65 °C.

2-{2-[2-(2-(*tert*-Butyldimethylsiloxy)ethoxy)ethoxy]ethoxy}ethyl 3,4,5-Tris[(4-(4′-(dodecyloxy)phenyl)benzyl)oxy]benzoate (12-12-Bp). The esterification of 1.90 g (1.56 mmol) of **8-12-Bp** with 0.576 g (1.87 mmol) of **11** was performed as described in the synthesis of **12-12-Nf** using 1,2-dichloroethane as solvent instead of CH$_2$Cl$_2$. The reaction was heated to reflux for 19 h and worked up. The crude product was chromatographed on basic Al$_2$O$_3$ using CH$_2$Cl$_2$ eluent and then recrystallized from hot acetone, resulting in 1.24 g (52%) of a white solid. ^{1}H NMR, δ (CDCl$_3$, TMS, ppm): 0.04 [s, 6H, OSi(CH_3)$_2$], 0.88 (overlapped m, 18H, CH_3, OSi(CH$_2$)$_2$C(CH_3)$_3$], 1.27 [m, 54H, (CH_2)$_9$], 1.86 (m, 6H, CH_2CH$_2$OAr), 3.52 (t, 2H, CH_2OSi, J = 5.4), 3.61−3.83 [m, 12H, CH_2O(CH_2CH_2O)$_2$CH_2], 3.99−4.05 (m, 6H, CH_2OAr), 4.46 (t, 2H, CO$_2$CH_2, J = 5.4), 5.17 (s, 6H, ArCH_2OAr), 6.88−6.98 (overlapped d, 6H, ArH *ortho* to CH$_2$O−), 7.42−7.57 (overlapped m, 20H, ArH *meta* to −CH$_2$OAr, *meta* to CH$_2$O−, *ortho* to CH$_2$OAr, *ortho* to CO$_2$CH$_2$). HPLC: >99%. Mp: 103−104.5 °C.

2-{2-[2-(2-Hydroxyethoxy)ethoxy]ethoxy}ethyl 3,4,5-Tris((6-(dodecyloxy)naphth-2-yl)methoxy)benzoate (13-12-Nf). The deprotection of **12-12-Nf** was perfomed using a modified literature procedure.[8] A 125 mL polypropylene flask containing a Teflon-coated magnetic stir bar was charged with 1.45 g (1.01 mmol) of **12-12-Nf** and 25 mL of dry THF. The flask was flushed with N$_2$ and closed with a rubber stopper attached to a N$_2$ line. The solution was cooled in an ice/H$_2$O bath and HF·Py (2.0 mL) was added dropwise. The ice/H$_2$O bath was removed and the reaction was stirred for an additional 30 min. TLC (2:1 hexanes/ethyl acetate) indicated complete deprotection. The reaction solution was diluted with 100 mL of Et$_2$O, and saturated NaHCO$_3$ solution was added cautiously with stirring until CO$_2$ evolution ceased. The two phases were separated, and the organic phase was washed with three 100 mL portions of H$_2$O and 50 mL of saturated NaCl and then dried over MgSO$_4$. The solution was filtered, and the solvent was removed using a rotary evaporator. The crude product was recrystallized from 1:1 hexanes/Et$_2$O and dried under high vacuum resulting in 1.26 g (95%) of a white solid. ^{1}H NMR, δ (CDCl$_3$, TMS, ppm): 0.88 (t, 9H, CH_3, J = 6.6), 1.27 [m, 54H, (CH_2)$_9$], 1.86 (m, 6H, CH_2CH$_2$OAr), 3.56−3.70 [m, 12H, (CH_2CH_2O)$_3$H], 3.83 (t, 2H, CO$_2$CH$_2$CH_2, J = 5.3), 4.08 (m, 6H, CH_2OAr), 4.45 (t, 2H, CO$_2$CH_2, J = 5.3), 5.27 (s, 6H, ArCH_2OAr), 6.99−7.17 (overlapped m, 6H, H5, H7), 7.35 (s, 2H, ArHCO$_2$CH$_2$), 7.40−7.52 [overlapped m, 5H, H3, H1 (*para* to CO$_2$CH$_2$), H4 (*para* to CO$_2$CH$_2$)], 7.62−7.82 [overlapped m, 7H, H1 (*para* to CO$_2$CH$_2$), H4 (*para* to CO$_2$CH$_2$), H8]. ^{13}C NMR, δ (CDCl$_3$, TMS, ppm): 14.1 (*C*H$_3$), 22.6 (CH$_3$*C*H$_2$), 26.6−31.9 [(*C*H$_2$)$_9$], 61.7 (*C*H$_2$OH), 64.1 (CO$_2$*C*H$_2$), 68.0 (*C*H$_2$ONpth), 69.2−70.2, 72.5 [*C*H$_2$(OC*H*$_2$*C*H$_2$)$_2$OC*H*$_2$], 71.6 (Ar*C*H$_2$OAr, *meta* to CO$_2$CH$_2$), 75.3 (Ar*C*H$_2$OAr *para* to CO$_2$CH$_2$), 106.4 (C5), 109.5 (*ortho* to CO$_2$CH$_2$), 118.8−119.3 (C7), 125.1 (*ipso* to CO$_2$CH$_2$), 126.0−129.4 (C1, C3, C4, C4′, C8), 131.7−132.5 (C2), 134.3 (C8′), 142.8 (*para* to CO$_2$CH$_2$), 152.7 (*meta* to CO$_2$CH$_2$), 157.4 (C6), 166.0 (*C*O$_2$CH$_2$). IR, ν_{max}(cm^{-1}): 3100−3600 (OH), 1705 (C=O). HPLC: >99%. TLC: R_f = 0 (2:1 hexanes/ethyl acetate). Thermal transitions and the corresponding enthalpy changes are reported in Table 4.1.

2-{2-[2-(2-Hydroxyethoxy)ethoxy]ethoxy}ethyl 3,4,5-Tris((6-(decyloxy)naphth-2-yl)methoxy)benzoate (13-10-Nf). The deprotection of **12-10-Nf** was performed as described in the synthesis of **13-12-Nf**. Deprotection of 2.60 g (1.92 mmol) of **12-10-Nf** resulted in 1.85 g (78%) of a white solid following recrystallization from 1:1 acetone/methanol. ^{1}H NMR, δ (CDCl$_3$, TMS, ppm): 0.88 (t, 9H, CH_3, J = 6.7), 1.27 [m, 42H, (CH_2)$_7$], 1.58 (s, CH$_2$O*H*, 1H), 1.85 (m, 6H, CH_2CH$_2$OAr), 3.56−3.71 [m, 12H, (CH_2CH_2O)$_3$H], 3.83 (t, 2H, CO$_2$CH$_2$CH_2, J = 5.3), 4.08 (m, 6H, CH_2OAr), 4.45 (t, 2H, CO$_2$CH_2, J = 5.3), 5.27 (s, 6H, ArCH_2OAr), 6.99−7.18 (overlapped m, 6H, H5, H7), 7.35 (s, 2H, ArHCO$_2$CH$_2$), 7.40−7.52 [overlapped m, 5H, H3, H1 (*para* to CO$_2$CH$_2$), H4 (*para* to CO$_2$CH$_2$)], 7.62−7.82 [overlapped m, 7H, H1 (*para* to CO$_2$CH$_2$), H4 (*para* to CO$_2$CH$_2$), H8]. ^{13}C NMR, δ (CDCl$_3$, TMS, ppm): 14.1 (*C*H$_3$), 22.6 (CH$_3$*C*H$_2$), 26.7−31.9 [(*C*H$_2$)$_7$], 61.7 (*C*H$_2$OH), 64.2 (CO$_2$*C*H$_2$), 68.0 (*C*H$_2$OAr), 69.2−70.2, 72.5 [*C*H$_2$(OC*H*$_2$*C*H$_2$)$_2$OC*H*$_2$], 71.6 (Ar*C*H$_2$OAr, *meta* to CO$_2$CH$_2$), 75.3 (Ar*C*H$_2$OAr *para* to CO$_2$CH$_2$), 106.4 (C5), 109.4 (*ortho* to CO$_2$CH$_2$), 118.9−119.3 (C7), 125.1 (*ipso* to CO$_2$CH$_2$), 126.0−129.4 (C1, C3, C4, C4′, C8), 131.7−132.5 (C2), 134.3 (C8′), 142.8 (*para* to CO$_2$CH$_2$), 152.7 (*meta* to CO$_2$CH$_2$), 157.4 (C6), 166.0 (*C*O$_2$CH$_2$). IR, ν_{max}(cm^{-1}): 3100−3600 (OH), 1705 (C=O). HPLC: >99%. TLC: R_f = 0 (2:1 hexanes/ethyl acetate). Thermal transitions and corresponding enthalpy changes are reported in Table 4.1.

2-{2-[2-(2-Hydroxyethoxy)ethoxy]ethoxy}ethyl 3,4,5-Tris((6-(tetradecyloxy)naphth-2-yl)methoxy)benzoate (13-14-Nf). The deprotection of **12-14-Nf** was performed as described in the synthesis of **13-12-Nf**. From 2.36 g (1.58 mmol) of **12-14-Nf**, 1.55 g (71%) of white crystals (after recrystallization from 1:1 acetone/methanol was obtained). ^{1}H NMR, δ (CDCl$_3$, TMS, ppm): 0.88 (t, 9H, CH_3, J = 6.5), 1.27 [m, 66H, (CH_2)$_{11}$], 1.58 (s, CH$_2$O*H*, 1H), 1.85 (m, 6H, CH_2CH$_2$OAr), 3.57−3.71 [m, 12H, (CH_2CH_2O)$_3$H], 3.83 (t, 2H, CO$_2$CH$_2$CH_2, J = 5.3), 4.08 (m, 6H, CH_2OAr), 4.45 (t, 2H, CO$_2$CH_2, J = 5.5), 5.27 (s, 6H, ArCH_2OAr), 7.00−7.20 (overlapped m, 6H, H5, H7), 7.35 (s, 2H, ArHCO$_2$CH$_2$), 7.40−7.52 [overlapped m, 5H, H3, H1 (*para* to CO$_2$CH$_2$), H4 (*para* to CO$_2$CH$_2$)], 7.62−7.82 [overlapped m, 7H, H1 (*para* to CO$_2$CH$_2$), H4 (*para* to CO$_2$CH$_2$), H8]. ^{13}C NMR, δ (CDCl$_3$, TMS, ppm): 14.1 (*C*H$_3$), 22.6 (CH$_3$*C*H$_2$), 26.7−32.0 [(*C*H$_2$)$_{11}$], 61.7 (*C*H$_2$OH), 64.2 (CO$_2$*C*H$_2$), 68.0 (*C*H$_2$OAr), 69.2−70.2, 72.5 [*C*H$_2$(OCH$_2$*C*H$_2$)$_2$OCH$_2$], 71.6 (Ar*C*H$_2$OAr, *meta* to CO$_2$CH$_2$), 75.3 (Ar*C*H$_2$OAr *para* to CO$_2$CH$_2$), 106.4 (C5), 109.4 (*ortho* to CO$_2$CH$_2$), 118.9−119.3 (C7), 125.1 (*ipso* to CO$_2$CH$_2$), 126.1−129.4 (C1, C3, C4, C4′, C8), 131.7−132.5 (C2), 134.3 (C8′), 142.8 (*para* to CO$_2$CH$_2$), 152.7 (*meta* to CO$_2$CH$_2$), 157.4 (C6), 166.0 (*C*O$_2$CH$_2$). HPLC: >99%. Thermal transitions and corresponding enthalpy changes are reported in Table 4.1.

2-{2-[2-(2-Hydroxyethoxy)ethoxy]ethoxy}ethyl 3,4,5-Tris((6-(hexadecyloxy)naphth-2-yl)methoxy)benzoate (13-16-Nf). The deprotection of **12-16-Nf** was performed as described in the synthesis of **13-12-Nf**. From 1.91 g (1.19 mmol) of **12-16-Nf**, 1.75 g (99%) of white crystals (following recrystallization from 1:1 acetone/methanol was obtained). ^{1}H NMR, δ (CDCl$_3$, TMS, ppm): 0.88 (t, 9H, CH_3, J = 6.6), 1.27 [m, 78H, (CH_2)$_{13}$], 1.58 (s, CH$_2$O*H*, 1H), 1.85 (m, 6H, CH_2CH$_2$OAr), 3.57−3.72 [m, 12H, (CH_2CH_2O)$_3$H], 3.82 (t, 2H, CO$_2$CH$_2$CH_2, J = 5.3), 4.08 (m, 6H, CH_2OAr), 4.45 (t, 2H, CO$_2$CH_2, J = 5.5), 5.27 (s, 6H, ArCH_2OAr), 7.00−7.19 (overlapped m, 6H, H5, H7), 7.36 (s, 2H, ArHCO$_2$CH$_2$), 7.41−7.52 [overlapped m, 5H, H3, H1 (*para* to CO$_2$CH$_2$), H4 (*para* to CO$_2$CH$_2$)], 7.62−7.82 [overlapped m, 7H, H1 (*para* to CO$_2$CH$_2$), H4 (*para* to CO$_2$CH$_2$), H8]. ^{13}C NMR, δ (CDCl$_3$, TMS, ppm): 14.1 (*C*H$_3$), 22.6 (CH$_3$*C*H$_2$), 26.7−32.1 [(*C*H$_2$)$_{13}$], 61.7 (*C*H$_2$OH), 64.2 (CO$_2$*C*H$_2$), 68.0 (*C*H$_2$OAr), 69.2−70.2, 72.5 [*C*H$_2$(OC*H*$_2$*C*H$_2$)$_2$OC*H*$_2$], 71.6 (Ar*C*H$_2$OAr, *meta* to CO$_2$CH$_2$), 75.3 (Ar*C*H$_2$OAr *para* to CO$_2$CH$_2$), 106.4 (C5), 109.4 (*ortho* to CO$_2$CH$_2$), 118.9−119.3 (C7), 125.1 (*ipso* to CO$_2$CH$_2$), 126.1−129.4 (C1, C3, C4, C4′, C8), 131.7−132.5 (C2), 134.3 (C8′), 142.8 (*para* to CO$_2$CH$_2$), 152.7 (*meta* to CO$_2$CH$_2$), 157.4 (C6), 166.0 (*C*O$_2$CH$_2$). HPLC: >99%. Thermal transitions and corresponding enthalpy changes are reported in Table 4.1.

2-{2-[2-(2-Hydroxyethoxy)ethoxy]ethoxy}ethyl 3,4,5-Tris[(4-(4′-dodecyloxy)phenyl)benzyl)oxy]benzoate (13-12-Bp). The deprotection of **12-12-Bp** was performed as described in the synthesis of **13-12-Nf**. Deprotection of 1.0 g (0.66 mmol) of **12-12-Bp** resulted in 0.87 g (94%) of a white solid. ^{1}H NMR, δ ($CDCl_3$, TMS, ppm): 0.88 (t, 9H, CH_3, J = 6.6), 1.27 [m, 54H, (CH_2)$_9$], 1.84 (overlapped m, 7H, CH_2CH$_2$-OAr, OH), 3.58−3.83 [m, 14H, CH_2O(CH_2CH_2O)$_2$CH_2CH_2], 3.95−4.05 (m, 6H, CH_2OAr), 4.45 (t, 2H, CO$_2$CH_2, J = 5.4), 5.18 (s, 6H, ArCH_2OAr), 6.88−7.00 (overlapped d, 6H, ArH *ortho* to CH$_2$O−), 7.42−7.59 (overlapped m, 20H, ArH *meta* to −CH$_2$OAr, *meta* to CH$_2$O−, *ortho* to CH$_2$OAr, *ortho* to CO$_2$-CH$_2$). ^{13}C NMR, δ($CDCl_3$, TMS, ppm): 14.1 (*C*H$_3$), 22.7 (CH$_3$*C*H$_2$), 26.1−31.9 [(*C*H$_2$)$_9$], 61.7 (*C*H$_2$OH), 64.2 (CO$_2$*C*H$_2$), 68.1 (*C*H$_2$OAr), 69.2−70.6, 72.5 [*C*H$_2$(O*C*H$_2$*C*H$_2$)$_2$O*C*H$_2$], 71.1 (Ar*C*H$_2$OAr, *meta* to CO$_2$CH$_2$), 75.0 (Ar*C*H$_2$OAr *para* to CO$_2$-CH$_2$), 109.4 (*ortho* to CO$_2$H), 114.8 (*ortho* to −OCH$_2$CH$_2$ on the biphenyl), 125.2 (*ipso* to CO$_2$CH$_2$), 126.2−126.7 (*meta* to −CH$_2$OAr on the biphenyl), 128.0−129.0 (*ortho* to −CH$_2$OAr on the biphenyl, *meta* to −OCH$_2$CH$_2$ on the biphenyl), 133.0 (*ipso* to −CH$_2$OAr on the biphenyl), 134.2−134.9 (*para* to −OCH$_2$CH$_2$ on the biphenyl, *para* to −CH$_2$OAr on the biphenyl), 140.6 (*para* to CO$_2$CH$_2$), 152.6 (*meta* to CO$_2$CH$_2$), 158.8 (*ipso* to −OCH$_2$CH$_2$ on the biphenyl), 166.0 (*C*O$_2$CH$_2$). IR, ν_{max}(cm^{-1}): 3200−3600 (OH), 1700 (C=O). TLC: R_f = 0 (2:1 hexanes/ethyl acetate). HPLC: >99%. Thermal transitions and corresponding enthalpy changes are recorded in Table 4.1.

2-{2-[2-(2-(Methacryloyloxy)ethoxy)ethoxy]ethoxy}-ethyl 3,4,5-Tris((6-(dodecyloxy)naphth-2-yl)oxy)benzoate (15-12-Nf). In a three-neck 50 mL round-bottom flask containing a Teflon-coated magnetic stirring bar was placed 1.2 g (0.9 mmol) of **13-12-Nf**, 8 mL of dry CH_2Cl_2, and 0.2 mL (1.4 mmol) of dry Et_3N. The flask was flushed with N_2 and attached to a N_2 line. A rubber septum and glass stopper were used to seal the flask. The reaction solution was cooled in an ice bath, and 0.15 mL (1.1 mmol) of methacryloyl chloride (**14**) was added dropwise via syringe. After 1 h, TLC analysis (2:1 hexanes/ethyl acetate) indicated complete conversion. The solvent was removed using a rotary evaporator, and the crude solid was chromatographed (neutral Al_2O_3, 2:1 hexanes/ethyl acetate). The resulting solid was dissolved in THF and precipitated into MeOH and then dried under high vacuum, resulting in 0.6 g (48%) of a white solid. ^{1}H NMR, δ ($CDCl_3$, TMS, ppm): 0.88 (t, 9H, CH_3, J = 6.7), 1.27 [m, 54H, (CH_2)$_9$], 1.80−1.92 [overlapped m, 9H, CH_2CH$_2$OAr, CH(CH_3)=CH$_2$], 3.63−3.72 [m, 10H, (CH_2CH_2O)$_2$CH_2], 3.80 (t, 2H, CO$_2$CH$_2$CH_2, J = 4.9), 4.08 (m, 6H, CH_2OAr), 4.27 [t, 2H, CH_2OC(O)C-(CH$_3$)=CH$_2$, J = 4.9], 4.47 (t, 2H, CO$_2$CH_2, J = 4.9), 5.26 (s, 6H, ArCH_2OAr), 5.55 [m, 1H, C(CH$_3$)=CH_2], 6.11 [s, 1H, C(CH$_3$)=CH_2], 6.98−7.17 (overlapped m, 6H, H5, H7), 7.36 (s, 2H, ArHCO$_2$CH$_2$), 7.40−7.52 [overlapped m, 5H, H3, H1 (*para* to CO$_2$CH$_2$), H4 (*para* to CO$_2$CH$_2$)], 7.62−7.82 [overlapped m, 7H, H1 (*para* to CO$_2$CH$_2$), H4 (*para* to CO$_2$CH$_2$), H8]. ^{13}C NMR, δ ($CDCl_3$, TMS, ppm): 14.1 (*C*H$_3$), 18.3 (CH$_2$=C(*C*H$_3$)-CO$_2$), 22.7 (CH$_3$*C*H$_2$), 26.1−31.9 [(*C*H$_2$)$_9$], 63.8 (*C*H$_2$OC(O)C-(CH$_3$)=CH$_2$), 64.2 (ArCO$_2$*C*H$_2$), 68.1 (*C*H$_2$ONpth), 69.1−70.6, [*C*H$_2$(OCH$_2$-*C*H$_2$)$_2$O*C*H$_2$], 71.6 (Npth*C*H$_2$OAr, *meta* to CO$_2$CH$_2$), 75.3 (Npth*C*H$_2$OAr *para* to CO$_2$CH$_2$), 106.4 (C5), 109.5 (*ortho* to CO$_2$CH$_2$), 118.9−119.3 (C7), 125.2 (*C*H$_2$=C(CH$_3$)C(O)), 125.6 (*ipso* to CO$_2$CH$_2$), 126.0−129.4 (C1, C3, C4, C4′, C8), 131.7−132.5 (C2), 134.3 (C8′), 136.0 (CH$_2$=*C*(CH$_3$)C(O)), 142.8 (*para* to CO$_2$CH$_2$), 152.7 (*meta* to CO$_2$CH$_2$), 157.2 (C6), 162.0 (CH$_2$O*C*(O)C(CH$_3$)=CH$_2$), 165.8 (*C*O$_2$CH$_2$). IR, ν_{max}(cm^{-1}): 1710 (C=O), 1630 (C=C). HPLC: >99%. TLC: R_f = 0.27 (2:1 hexanes/ethyl acetate). Mp: 55 °C.

2-{2-[2-(2-(Methacryloyloxy)ethoxy)ethoxy]ethoxy}-ethyl 3,4,5-Tris((6-(decyloxy)naphth-2-yl)methoxy)benzoate (15-10-Nf). The esterification of **13-10-Nf** with methacryloyl chloride (**14**) was performed as described in the synthesis of **15-12-Nf**. From 1.50 g (1.21 mmol) of **13-10-Nf** and 0.20 mL of methacryloyl chloride (**14**) was obtained 0.78 g (50%) of a white solid. ^{1}H NMR, δ ($CDCl_3$, TMS, ppm): 0.88 (t, 9H, CH_3, J = 6.7), 1.27 [m, 42H, (CH_2)$_7$], 1.80−1.92 [overlapped m, 9H, CH_2CH$_2$OAr, CH(CH_3)=CH$_2$], 3.62−3.72 [m, 10H, (CH_2CH_2O)$_2$CH_2], 3.81 (t, 2H, CO$_2$CH$_2$CH_2, J = 4.9), 4.08 (m, 6H, CH_2OAr), 4.27 [t, 2H, CH_2OC(O)C(CH$_3$)=CH$_2$, J = 4.9], 4.46 (t, 2H, CO$_2$CH_2, J = 4.9), 5.26 (s, 6H, ArCH_2OAr), 5.55 [m, 1H, C(CH$_3$)=CH_2], 6.11 [s, 1H, C(CH$_3$)=CH_2], 6.98−7.17 (overlapped m, 6H, H5, H7), 7.36 (s, 2H, ArHCO$_2$CH$_2$), 7.40−7.52 [overlapped m, 5H, H3, H1 (*para* to CO$_2$CH$_2$), H4 (*para* to CO$_2$CH$_2$)], 7.62−7.82 [overlapped m, 7H, H1 (*para* to CO$_2$CH$_2$), H4 (*para* to CO$_2$CH$_2$), H8]. ^{13}C NMR, δ ($CDCl_3$, TMS, ppm): 14.1 (*C*H$_3$), 18.2 (CH$_2$=C(*C*H$_3$)CO$_2$), 22.7 (CH$_3$*C*H$_2$), 26.1−31.9 [(*C*H$_2$)$_7$], 63.8 (*C*H$_2$OC(O)C(CH$_3$)=CH$_2$), 64.2 (ArCO$_2$*C*H$_2$), 68.1 (*C*H$_2$ONpth), 69.1−70.6, [*C*H$_2$(OCH$_2$-*C*H$_2$)$_2$O*C*H$_2$], 71.6 (Npth*C*H$_2$OAr, *meta* to CO$_2$CH$_2$), 75.3 (Npth*C*H$_2$OAr *para* to CO$_2$CH$_2$), 106.4 (C5), 109.5 (*ortho* to CO$_2$CH$_2$), 118.9−119.3 (C7), 125.2 (*C*H$_2$=C(CH$_3$)C(O)), 125.6 (*ipso* to CO$_2$CH$_2$), 126.1−129.4 (C1, C3, C4, C4′, C8), 131.7−132.5 (C2), 134.3 (C8′), 136.0 (CH$_2$=*C*(CH$_3$)C(O)), 142.8 (*para* to CO$_2$CH$_2$), 152.7 (*meta* to CO$_2$CH$_2$), 157.2 (C6), 161.9 (CH$_2$O*C*(O)C(CH$_3$)=CH$_2$), 165.8 (*C*O$_2$CH$_2$). IR, ν_{max}(cm^{-1}): 1710 (C=O), 1630 (C=C). HPLC: >99%. TLC: R_f = 0.25 (2:1 hexanes/ethyl acetate). Mp: 51−52 °C.

2-{2-[2-(2-(Methacryloyloxy)ethoxy)ethoxy]ethoxy}-ethyl 3,4,5-Tris((6-(tetradecyloxy)naphth-2-yl)methoxy)-benzoate (15-14-Nf). The esterification of **13-14-Nf** with methacryloyl chloride (**14**) was performed as described in the synthesis of **15-12-Nf**. From 1.20 g (0.855 mmol) of **13-14-Nf** and 0.10 mL methacryloyl chloride (**14**) was obtained 0.65 g (52%) of a white solid. ^{1}H NMR, δ ($CDCl_3$, TMS, ppm): 0.88 (t, 9H, CH_3, J = 6.8), 1.27 [m, 66H, (CH_2)$_{11}$], 1.80−1.92 [overlapped m, 9H, CH_2CH$_2$OAr, CH(CH_3)=CH$_2$], 3.61−3.72 [m, 10H, (CH_2CH_2O)$_2$CH_2], 3.82 (t, 2H, CO$_2$CH$_2$CH_2, J = 4.9), 4.08 (m, 6H, CH_2OAr), 4.27 [t, 2H, CH_2OC(O)C(CH$_3$)=CH$_2$, J = 4.9], 4.45 (t, 2H, CO$_2$CH_2, J = 4.9), 5.26 (s, 6H, ArCH_2OAr), 5.55 [m, 1H, C(CH$_3$)=CH_2], 6.11 [s, 1H, C(CH$_3$)=CH_2], 6.98−7.17 (overlapped m, 6H, H5, H7), 7.36 (s, 2H, ArHCO$_2$CH$_2$), 7.41−7.52 [overlapped m, 5H, H3, H1 (*para* to CO$_2$CH$_2$), H4 (*para* to CO$_2$CH$_2$)], 7.62−7.82 [overlapped m, 7H, H1 (*para* to CO$_2$CH$_2$), H4 (*para* to CO$_2$CH$_2$), H8]. ^{13}C NMR, δ ($CDCl_3$, TMS, ppm): 14.1 (*C*H$_3$), 18.2 (CH$_2$=C(*C*H$_3$)CO$_2$), 22.7 (CH$_3$*C*H$_2$), 26.0−32.0 [(*C*H$_2$)$_{11}$], 63.8 (*C*H$_2$OC(O)C(CH$_3$)=CH$_2$), 64.2 (ArCO$_2$*C*H$_2$), 68.1 (*C*H$_2$ONpth), 69.1−70.6, [*C*H$_2$(OCH$_2$-*C*H$_2$)$_2$O*C*H$_2$], 71.6 (Npth*C*H$_2$OAr, *meta* to CO$_2$CH$_2$), 75.3 (Npth*C*H$_2$OAr *para* to CO$_2$CH$_2$), 106.4 (C5), 109.5 (*ortho* to CO$_2$CH$_2$), 118.9−119.3 (C7), 125.2 (*C*H$_2$=C(CH$_3$)C(O)), 125.6 (*ipso* to CO$_2$CH$_2$), 126.1−129.4 (C1, C3, C4, C4′, C8), 131.7−132.5 (C2), 134.3 (C8′), 136.0 (CH$_2$=*C*(CH$_3$)C(O)), 142.8 (*para* to CO$_2$CH$_2$), 152.7 (*meta* to CO$_2$CH$_2$), 157.2 (C6), 161.9 (CH$_2$O*C*(O)C(CH$_3$)=CH$_2$), 165.8 (*C*O$_2$CH$_2$). HPLC: >99%. Mp: 60−61 °C.

2-{2-[2-(2-(Methacryloyloxy)ethoxy)ethoxy]ethoxy}-ethyl 3,4,5-Tris((6-(hexadecyloxy)naphth-2-yl)methoxy)-benzoate (15-16-Nf). The esterification of **13-16-Nf** with methacryloyl chloride (**14**) was performed as described in the synthesis of **15-12-Nf**. From 1.72 g (1.16 mmol) of **13-16-Nf** and 0.14 mL methacryloyl chloride (**14**) was obtained 0.82 g (45%) of a white solid. ^{1}H NMR, δ ($CDCl_3$, TMS, ppm): 0.88 (t, 9H, CH_3, J = 6.9), 1.27 [m, 78H, (CH_2)$_{13}$], 1.80−1.92 [overlapped m, 9H, CH_2CH$_2$OAr, CH(CH_3)=CH$_2$], 3.61−3.72 [m, 10H, (CH_2CH_2O)$_2$CH_2], 3.82 (t, 2H, CO$_2$CH$_2$CH_2, J = 4.9), 4.09 (m, 6H, CH_2OAr), 4.27 [t, 2H, CH_2OC(O)C(CH$_3$)=CH$_2$, J = 4.8], 4.45 (t, 2H, CO$_2$CH_2, J = 4.9), 5.26 (s, 6H, ArCH_2OAr), 5.55 [m, 1H, C(CH$_3$)=CH_2], 6.11 [s, 1H, C(CH$_3$)=CH_2], 6.97−7.17 (overlapped m, 6H, H5, H7), 7.36 (s, 2H, ArHCO$_2$CH$_2$), 7.42−7.52 [overlapped m, 5H, H3, H1 (*para* to CO$_2$CH$_2$), H4 (*para* to CO$_2$CH$_2$)], 7.62−7.82 [overlapped m, 7H, H1 (*para* to CO$_2$CH$_2$), H4 (*para* to CO$_2$CH$_2$), H8]. ^{13}C NMR, δ ($CDCl_3$, TMS, ppm): 14.1 (*C*H$_3$), 18.2 (CH$_2$=C(*C*H$_3$)CO$_2$), 22.7 (CH$_3$*C*H$_2$), 26.0−32.0 [(*C*H$_2$)$_{13}$], 63.8 (*C*H$_2$OC(O)C(CH$_3$)=CH$_2$), 64.2 (ArCO$_2$*C*H$_2$), 68.1 (*C*H$_2$ONpth), 69.1−70.6, [*C*H$_2$(OCH$_2$-*C*H$_2$)$_2$O*C*H$_2$], 71.6 (Npth*C*H$_2$OAr, *meta* to CO$_2$CH$_2$), 75.3 (Npth*C*H$_2$OAr *para* to CO$_2$CH$_2$), 106.4 (C5), 109.5 (*ortho* to CO$_2$CH$_2$), 118.9−119.2 (C7), 125.2 (*C*H$_2$=C(CH$_3$)C(O)), 125.6 (*ipso* to CO$_2$CH$_2$), 126.1−129.4 (C1, C3, C4, C4′, C8), 131.7−132.5 (C2), 134.3 (C8′), 136.0 (CH$_2$=*C*(CH$_3$)C(O)), 142.8 (*para* to CO$_2$CH$_2$), 152.7 (*meta* to CO$_2$CH$_2$), 157.2 (C6), 161.9 (CH$_2$O-*C*(O)C(CH$_3$)=CH$_2$), 165.8 (*C*O$_2$CH$_2$). HPLC: >99%. Mp: 67−68 °C.

2-{2-[2-(2-(Methacryloyloxy)ethoxy)ethoxy]ethoxy}-ethyl 3,4,5-Tris[(4-(4′-(dodecyloxy)phenyl)benzyl)oxy]-benzoate (15-12-Bp). The esterification of **13-12-Bp** with methacryloyl chloride (**14**) was performed as described in the synthesis of **15-12-Nf**. From 0.80 g (0.59 mmol) of **13-12-Bp** and 0.20 mL of methacryloyl chloride (**14**) was obtained 0.40 g (46%) of a white solid. ^{1}H NMR, δ ($CDCl_3$, TMS, ppm): 0.88 (t, 9H, C*H*$_3$, J = 6.6), 1.27 [m, 54H, (C*H*$_2$)$_9$], 1.84 (overlapped m, 7H, C*H*$_2$CH$_2$OAr, O*H*), 3.58−3.83 [m, 14H, C*H*$_2$O(C*H*$_2$-C*H*$_2$O)$_2$C*H*$_2$C*H*$_2$], 3.95−4.05 (m, 6H, C*H*$_2$OAr), 4.45 (t, 2H, CO$_2$C*H*$_2$, J = 5.4), 5.18 (s, 6H, ArC*H*$_2$OAr), 6.88−7.00 (overlapped d, 6H, Ar*H ortho* to CH$_2$O), 7.42−7.59 (overlapped m, 20H, Ar*H meta* to −CH$_2$OAr, *meta* to CH$_2$O−, *ortho* to CH$_2$-OAr, *ortho* to CO$_2$CH$_2$). IR, ν_{max}(cm^{-1}): 1710 (C═O), 1630 (C═C). HPLC: >99%.

Poly(2-{2-[2-(2-(methacryloyloxy)ethoxy)ethoxy]-ethoxy}ethyl-3,4,5 tris((6-(dodecyloxy)naphth-2-yl)-methoxy)benzoate) (16-12-Nf). A 25 mL Schlenk tube containing a Teflon-coated magnetic stirring bar was charged with 0.41 g (0.30 mmol) of **15-12-Nf**, 0.004 g (1 wt %) of AIBN, and 0.9 mL of benzene and sealed with a rubber septum. The solution was subjected to five freeze−pump−thaw cycles, sealed, and stirred at 60 °C for 20 h. GPC analysis indicated 89% conversion. The crude reaction mixture was passed through a short neutral Al_2O_3 column to remove residual monomer. The resulting solid was dissolved in THF and precipitated into MeOH and then dried under high vacuum, yielding 0.33 g (80%) of solid polymer. Molecular weight, thermal transitions and corresponding enthalpy changes are reported in Table 4.1.

Poly(2-{2-[2-(2-(methacryloyloxy)ethoxy)ethoxy]-ethoxy}ethyl 3,4,5-tris((6-(decyloxy)naphth-2-yl)methoxy)-benzoate) (16-10-Nf). Polymerization of **15-10-Nf** was performed as described for **15-12-Nf**. From 0.66 g (0.50 mmol) **15-10-Nf** was obtained 0.45 g (68%) of a white solid. Molecular weight, thermal transitions, and corresponding enthalpy changes are reported in Table 1.

Poly(2-{2-[2-(2-(methacryloyloxy)ethoxy)ethoxy]-ethoxy}ethyl 3,4,5-tris((6-(tetradecyloxy)naphth-2-yl)-methoxy)benzoate) (16-14-Nf). Polymerization of **15-14-Nf** was performed as for **15-12-Nf**. From 0.49 g (0.33 mmol) **15-14-Nf** was obtained 0.30 g (61%) of a white polymeric solid. Molecular weight, thermal transitions, and corresponding enthalpy changes are reported in Table 1.

Poly(2-{2-[2-(2-(methacryloyloxy)ethoxy)ethoxy]-ethoxy}ethyl 3,4,5-tris((6-(hexadecyloxy)naphth-2-yl)-methoxy)benzoate) (16-16-Nf). The polymerization of **15-16-Nf** was performed as described for **15-12-Nf**. From 0.41 g (0.26 mmol) of **15-16-Nf** was obtained 0.18 g (44%) of a white polymeric solid. Molecular weight, thermal transitions, and corresponding enthalpy changes are reported in Table 1.

Poly(2-{2-[2-(2-(methacryloyloxy)ethoxy)ethoxy]-ethoxy}ethyl 3,4,5-tris[(4-(4′-dodecyloxy)phenyl)benzyl)-oxy]benzoate) (16-12-Bp). The polymerization of **15-12-Bp** was performed as described in the case of **15-12-Nf**. From 0.11 g (0.075 mmol) of **15-12-Bp** was obtained 0.055 g (50%) of a white solid. Molecular weight, thermal transitions, and corresponding enthalpy changes are reported in Table 1.

Acknowledgment. Financial support by the National Science Foundation (DMR-9708581) is gratefully acknowledged.

References and Notes

(1) For selected publications from our laboratory on the self-assembly of taper shaped monodendrons evolved from phasmidic and hemiphasmidic architectures and of their supramolecular assemblies and polymers, see: (a) Percec, V.; Johansson, G.; Ungar, G.; Zhou, J. P. *J. Am. Chem. Soc.* **1996**, *118*, 9855. (b) Percec, V.; Johansson, G.; Ungar, G.; Zhou, J. P. *Macromolecules* **1996**, *29*, 646. (c) Percec, V.; Schlueter, D.; Kwon, Y.-K.; Blackwell, J.; Möller, M.; Slangen, P. J. *Macromolecules* **1995**, *28*, 8807. (d) Percec, V.; Johannson, G.; Heck, J.; Ungar, G.: Batty, S. V. *J. Chem. Soc., Perkin Trans. 1* **1993**, 1411. (e) Johansson, G.; Percec, V.; Ungar, G.; Abramic, D. *J. Chem. Soc., Perkin Trans. 1* **1994**, 447. (f) Percec, V.; Heck, J.; Tomazos, D.; Falkenberg, F.; Blackwell, H.; Ungar, G. *J. Chem. Soc., Perkin Trans. 1* **1993**, 2799. (g) Percec, V.; Heck, J.; Tomazos, D.; Ungar, G. *J. Chem. Soc., Perkin Trans. 2* **1993**, 2381. (h) Percec, V.; Tomazos, D.; Heck, J.; Blackwell, H.; Ungar, G. *J. Chem. Soc., Perkin Trans. 2* **1994**, 31. (i) Hudson, S. D.; Jung, H.-T.; Percec, V.; Cho, W.-D.; Johansson, G.; Ungar, G.; Balagurusamy V. S. K. *Science* **1997**, *278*, 449.

(2) For some brief reviews from our laboratory on the self-assembly of taper-shaped monodendrons, see: (a) Percec, V.; Johansson, G. In *Macromolecular Design of Polymeric Materials*; Hatada, K., Kitayama, T., Vogl, O., Eds.; M. Dekker: New York, 1997. (b) Percec, V.; Johansson, G.; Schlueter, D.; Ronda, J. C.; Ungar, G. *Macromol. Symp.* **1996**, *101*, 43. (c) Percec, V.; Heck, J.; Johansson, G.; Tomazos, D.; Ungar, G. *Macromol. Symp.* **1994**, *77*, 237. (d) Percec, V.; Heck, J.; Johansson, G.; Tomazos, D.; Kawasumi, M.; Chu, P.; Ungar, G. *J. Macromol. Sci.—Pure Appl. Chem.* **1994**, *A31*, 1719. (e) Percec, V.; Heck, J.; Johansson, G.; Tomazos, D.; Kawasumi, M.; Chu, P.; Ungar, G. *Mol. Cryst. Liq. Cryst.* **1994**, *254*, 137. (f) Percec, V.; Ahn, C.-H.; Cho, W.-D.; Johansson, G.: Schlueter, D. *Macromol. Chem.* **1997**, *118*, 33.

(3) (a) Percec, V.; Schlueter, D.; Ronda, J. C.; Johansson, G.; Ungar, G.; Zhou, J. P. *Macromolecules* **1996**, *29*, 1464. (b) Kwon, Y.-K.; Chvalun, S.; Blackwell, J.; Percec, V.; Heck, J. A. *Macromolecules* **1995**, *28*, 6129. (c) Kwon, Y.-K.; Chvalun, S.; Schneider, A. I.; Blackwell, J.; Percec, V.; Heck, J. A. *Macromolecules* **1994**, *27*, 6129. (d) Percec, V.; Schlueter, D. *Macromolecules* **1997**, *30*, 5783. (e) Percec, V.; Lee, M.; Heck, J. A.; Blackwell, H.; Alvarez-Castillo, A. *J. Mater. Chem.* **1992**, *2*, 1033. (f) Percec, V.; Lee., M.; Heck, J.; Blackwell, H. E.; Ungar, G.; Alvarez-Castillo, A. *J. Mater. Chem.* **1992**, *2*, 931. (g) Percec, V.; Heck, J. Ungar, G. *Macromolecules* **1991**, *24*, 4957. (h) Percec, V.; Heck, J.; *J. Polym. Sci., Part A: Polym. Chem.* **1991**, *29*, 591.

(4) For the pioneering report on the synthesis of cylindrical dendrimers, see: (a) Tomalia, D. A.; Kirchhoff. U. S. Patent 1987, 4,694,064. For recent strategies to cylindrical shaped and other structures from polymers containing Fréchet-type monodendrons as side groups, see: (b) Fréchet, J. M. J.; Gitsov, I. *Macromol. Symp.* **1995**, *98*, 44. (c) Karakaya, B.; Claussen, W.; Gessler, K.; Saenger, W.; Schlüter, A.-D. *J. Am. Chem. Soc.* **1997**, *119*, 3296 and references therein; (d) Niggemann, M.; Ritter, H. *Acta Polym.* **1996**, *47* 351 and references therein; (e) Chen, Y.-M.; Chen, C.-F.; Liu, W.-H.; Li, F.-Y.; Xi, F. *Macromol. Rapid Commun.* **1996**, *17*, 40. (f) Kaneko, T.; Horie, T.; Asano, M.; Toshiki, A.; Oikawa, E. *Macromolecules* **1997**, *30*, 3118 and references therein.

(5) For examples of polymacromonomers containing polystyrene side groups, see: (a) Wintermantel, M.; Gerle, M.; Fischer, K.; Schmidt, M.; Wataoka, I.; Urakawa, H.; Kajiwara, K.; Tsukahara, Y. *Macromolecules* **1996**, *29*, 978. (b) Wintermantel, M.; Fischer, K.; Gerle, M.; Ries, R.; Schmidt, M.; Kajiwara, K.; Urakawa, H.; Wataoka, I. *Angew. Chem., Int. Ed. Engl.* **1995**, *34*, 1472.

(6) Percec, V.; Oda, H.; Rinaldi, P. L.; Hensley, D. R. *Macromolecules* **1994**, *27*, 12.

(7) Chandhary, S. K.; Hernandez, O. *Tetrahedron Lett.* **1979**, 99.

(8) Nicolaou, K. C.; Webber, S. E. *Synthesis* **1986**, 453.

(9) Malthête, J.; Collet, A.; Levelut, A. M. *Liq. Cryst.* **1989**, *5*, 123.

(10) Ungar, G.; Abramic, D.; Percec, V.; Heck, J. A. *Liq. Cryst.* **1996**, *21*, 73.

(11) Percec, V.; Schlueter, D.; Ungar, G. Unpublished results.

(12) Wilds, A. L.; Shunk, C. H. *J. Am. Chem. Soc.* **1950**, *72*, 2388.

(13) Hanabusa, K.; Tanaka, O.; Koyama, T.; Kurose, A.; Shirai, H.; Hayakawa, T.; Hojo, N. *Polym. J. (Jpn.)* **1988**, *20*, 861.

MA971459P